E7 oncoprotein from human papillomavirus 16 alters claudins expression and the sealing of epithelial tight junctions

PERLA YACELI UC[1,2], JAEL MIRANDA[1], ARTURO RAYA-SANDINO[1], LOURDES ALARCÓN[1], MARÍA LUISA ROLDÁN[1], RODOLFO OCADIZ-DELGADO[3], ENOC MARIANO CORTÉS-MALAGÓN[4], BIBIANA CHÁVEZ-MUNGUÍA[5], GEORGINA RAMÍREZ[6], RENÉ ASOMOZA[6], LIORA SHOSHANI[1], PATRICIO GARIGLIO[3] and LORENZA GONZÁLEZ-MARISCAL[1]

[1]Department of Physiology, Biophysics and Neuroscience, Center for Research and Advanced Studies, Mexico City 07360; [2]Faculty of Medicine, National University of Mexico, Mexico City 04360; [3]Department of Genetics and Molecular Biology, Center for Research and Advanced Studies, Mexico City 07360; [4]Research Unit on Genetics and Cancer, Research Division, Hospital Juárez de México, Mexico City 07760; [5]Department of Infectomics and Molecular Pathogenesis, Center for Research and Advanced Studies; [6]Department of Electrical Engineering, Center for Research and Advanced Studies, Mexico City 07360, Mexico

Received January 26, 2020; Accepted April 16, 2020

DOI: 10.3892/ijo.2020.5105

Abstract. Tight junctions (TJs) are cell-cell adhesion structures frequently altered by oncogenic transformation. In the present study the role of human papillomavirus (HPV) 16 E7 oncoprotein on the sealing of TJs was investigated and also the expression level of claudins in mouse cervix and in epithelial Madin-Darby Canine Kidney (MDCK) cells. It was found that there was reduced expression of claudins -1 and -10 in the cervix of 7-month-old transgenic K14E7 mice treated with 17β-estradiol (E_2), with invasive cancer. In addition, there was also a transient increase in claudin-1 expression in the cervix of 2-month-old K14E7 mice, and claudin-10 accumulated at the border of cells in the upper layer of the cervix in FvB mice treated with E_2, and in K14E7 mice treated with or without E_2. These changes were accompanied by an augmented paracellular permeability of the cervix in 2- and 7-month-old FvB mice treated with E_2, which became more pronounced in K14E7 mice treated with or without E_2. In MDCK cells the stable expression of E7 increased the space between adjacent cells and altered the architecture of the monolayers, induced the development of an acute peak of transepithelial electrical resistance accompanied by a reduced expression of claudins -1, -2 and -10, and an increase in claudin-4. Moreover, E7 enhances the ability of MDCK cells to migrate through a 3D matrix and induces cell stiffening and stress fiber formation. These observations revealed that cell transformation induced by HPV16 E7 oncoprotein was accompanied by changes in the pattern of expression of claudins and the degree of sealing of epithelial TJs.

Correspondence to: Dr Lorenza González-Mariscal, Department of Physiology, Biophysics and Neuroscience, Center for Research and Advanced Studies, Avenue IPN 2508, Mexico City 07360, Mexico
E-mail: lorenza@fisio.cinvestav.mx

Key words: tight junctions, human papillomavirus, HPV E7, claudins, paracellular permeability

Introduction

Cervical cancer is the fourth most common cancer in women and the fourth leading cause of cancer-associated mortality in women (with incidence and mortality rates of 6.6 and 7.5% considering the 10 most common cancers in women in 2018, respectively), with an estimated 570,000 cases and 311,000 deaths worldwide in 2018 (1). Moreover, in regions of the world with low (e.g. Niger, Chad, Sierra Leone, Gambia and Nigeria) and medium (Paraguay, Egypt, Vietnam, El Salvador, Nicaragua, Zambia and Pakistan) human development index, cervical cancer has the second highest incidence (18.2%) and mortality (12%) rates, behind breast cancer (1). In the USA 13,800 new cases and 4,290 cervical cancer-associated deaths have been estimated for 2020, and the probability, from birth to death, of developing invasive cervical cancer from 2014 to 2016 was of 0.6% (2). Since the mid-1970s cancer survival has improved in the USA for all of the most common cancers (e.g. lung and bronchus, colon and rectum, breast, prostate, oral cavity and pharynx, esophagus, stomach, pancreas, liver, kidney, urinary bladder, melanoma, ovary and thyroid), except those of the uterine cervix and uterine corpus (3). In cervical cancer the 5-year relative survival rate for all races, according to the stage at diagnosis, was 92%, 56% and 17%, for localized, regional and distant lesions, respectively (2). Moreover, cervical cancer remains the second leading cause of cancer-associated death in women aged 20 to 39 years in the USA (2).

Infection with a subtype of the human papillomavirus, known as high-risk (HR), is the most common cause of

cervical cancer (4). However, not all women infected with HR-HPV will develop cervical cancer, as this disease develops over 2 decades following exposure to these viruses and might require additional contributing factors, including tobacco smoke (5), parity (6,7), estrogens (8), oral contraceptives (9), immune deficiencies, such as human immunodeficiency virus-seropositive women (10), genetic polymorphisms (11), epigenetic regulation of costimulatory factors Tim-3 and galectin-9 (12) and methylation sensitivity of the enhancer from HPV16 (13). Dietary factors also appear to play a role, as a diet rich in plant-based nutrients, which increases dietary fiber, vitamins -C, -E, -A, α- and β-carotenes and lutein, has been found to reduce the risk of cervical cancer (14,15).

HPVs are DNA viruses containing two genes, which are expressed early named E6 and E7, which in the high-risk viral types encode proteins that promote cervical carcinogenesis (16). E6 and E7 oncoproteins associate with and inactivate the tumor suppressor proteins p53 (17) and retinoblastoma (Rb) (18), respectively. Employing chemical carcinogens in the K14E7 transgenic mouse, E7 was found to promote the formation of benign tumors in the skin, while in the transgenic mice K14E6 treated with these carcinogens, E6 accelerate the progression of the benign tumors to the malignant state (16). However, in the cervix, E7 increased cell proliferation and generated micro-invasive cervical cancers, while E6 did not produce neoplasia or cancer even following 17β-estradiol (E_2) treatment, which is a contributing factor for cervical cancer, and was delivered in continuous release pellets implanted in the dorsal skin (8,19). The co-expression of E6 and E7 in double transgenic mice (K14-E6:E7) revealed that E6 modulated the malignant phenotype produced by E7, causing micro-invasive cervical cancers to be dispersed over a larger area of cervical stromal tissue (19). E_2 treatment is required not only for the genesis of cervical cancer (20,21) but also for its persistence and continued development (22).

The disassembly of the TJ, which is a cell-cell adhesion structure characteristic of epithelial cells, constitutes one of the earliest steps in cell transformation (23,24). However, its role in the development of cervical cancer has not been elucidated, therefore further investigation was performed in the present study. TJs are comprised of a complex group of molecules, including the peripheral proteins, cingulin, ZO-1, -2 and -3 and the integral proteins, claudins, occludin and JAMs. While numerous TJ proteins are downregulated during cell transformation (e.g. ZO-1, -2, and -3, occludin, JAM-A and MUPP1), others are overexpressed (e.g. claudins -2, -3 and -4), even though they are no longer present at the cell borders (23). With respect to claudins, there are differences in expression levels of the protein in different tissues and different types of cancer. For example, in lung squamous cell carcinomas claudins -1, -2, -4 and -7 are expressed, while claudins -2, -3, -4, -5 and -7 are expressed in lung adenocarcinomas, and claudin-4 was found to be expressed in lung large cell carcinomas express. Claudin-1 is expressed in esophageal squamous cell carcinomas, while in the adenocarcinoma form of the disease claudins -2, -3, -4, and -7 are expressed. Claudins -1, -4, -5 and -7 are expressed in the squamous cell carcinomas found in the oral cavity, while claudin-1 is expressed in the low mucoepidermoid carcinoma, and claudin-3 is expressed in the high mucoepidermoid carcinoma (23). Therefore the expression of claudins is a useful molecular tool for distinguishing between different types of tumors and for the prediction of patient survival rates. For example, claudin-6 is the most distinctive molecular marker of atypical teratoid/rhabdoid tumors, which are highly aggressive malignant central nervous system tumors of children, in comparison to other brain tumors, such as choroid plexus papilloma, ependymoma, large-cell medulloblastoma, classic medulloblastoma and pediatric glioblastoma (25).

In our previous study claudin-4 expression was found to increase in the cervix of K14E7 transgenic mice compared with that in non-transgenic mice, particularly in the presence of E_2 (26). In the present study the impact of the E7 oncoprotein on the expression levels of claudins -1 and -10 in the murine cervix was investigated, as the expression of claudin-1 has been found to decrease in breast carcinomas, stage II colon cancer, lymph node metastasis in colon carcinomas, colon mucinous carcinomas, lung adenocarcinomas, prostate adenocarcinomas, pancreatic endocrine tumors, gastric cancer, type I endometrial carcinomas, hepatocellular carcinomas, kidney clear cell carcinomas, papillary urothelial neoplasms of low malignant potential and low grade urothelial cell carcinomas, thyroid undifferentiated carcinomas and thyroid medullary carcinomas, while it is overexpressed in colorectal cancer, in the early phase of carcinogenesis in cervical intraepithelial lesions, esophageal squamous cell carcinoma, squamous cell carcinoma of the tongue, low grade mucoepidermoid carcinoma of minor salivary glands, and in melanoma (23). With regards to claudin-10, its expression was reduced in the biliary tract, breast carcinomas and in lung adenocarcinomas of the invasive type (23,24); however, it was increased in chicken ovarian cancer (27), hepatocellular carcinoma (28) and papillary thyroid cancer (29). To further confirm the results, the impact of the stable expression of the E7 oncoprotein in Madin-Darby Canine Kidney (MDCK) cells was also investigated, including monolayer morphology, transepithelial electrical resistance (TER), claudin expression, invasive properties and cell stiffness. The results indicate that E7 perturbs the expression pattern of claudins and the degree of sealing of TJs in the cervix, and in MDCK cells, and also alters the cytoarchitecture of the cervix and MDCK monolayer, induces migration of MDCK cells in three-dimensional (3D) cultures and triggers the stiffening of their apical membrane.

Materials and methods

Mouse model and hormone treatment. The K14E7 transgenic mice were a gift of Dr Paul F. Lambert (Department of Oncology, McArdle Laboratory for Cancer Research, University of Wisconsin, Madison, WI, USA) and were backcrossed in the FvB background, maintained and used as heterozygotes in further experiments. The FvB mice, used as the control group, were obtained from the animal facility of the Center for Research and Advanced Studies, Mexico. FvB and K14E7 transgenic female mice were housed in cages with double air filtration (HEPA level 99% of particles) and maintained at 20-22˚C, under a 12 h dark-light cycles with food and water *ad libitum*. Animals were sacrificed by cervical dislocation at 2-, 4- and 7-months of age. Hormone treatment was performed with continuous release pellets delivering 0.05 mg

of E_2 over 60 days (cat. no. SE-121; Innovative Research of America). Pellets were implanted in the dorsal skin of 1-month-old virgin female transgenic and non-transgenic mice. Mice sacrificed at 4-months of age received two E_2 pellets: one at the first month of age and the other at the 3rd month of age; whereas mice sacrificed at 7-months of age received an additional third pellet at the 5th month of age. A total of 42 mice were used in the study: 5 FvB mice, and 3 K14E7 at each age (2-, 4- and 7-months of age) were analyzed and 3 FvB and K14E7 mice treated with E_2 were also used for each age group (2-, 4- and 7-months of age). The weight of the FvB and K14E7 mice was similar to what had been previously reported (20, 26 and 30, and 18, 23 and 26 g for 2-, 4- and 7-month-old FvB and K14E7 mice, respectively) (30).

Cell culture. Epithelial MDCK cells were obtained from the American Type Culture Collection (cat. no. CCL-34). Cells between the 60th and 90th passage were grown at 36.5˚C in disposable plastic bottles in a humidified atmosphere with 5% CO_2 in DMEM (cat. no. 12800-082; Gibco; Thermo Fisher Scientific, Inc.) with 100 U/ml penicillin-streptomycin (cat. no. A-01; In Vitro, S.A; www.invitro.com.mx) and 10% fetal bovine serum (cat. no. S1650-500; Biowest). Cells were harvested with trypsin-EDTA (cat. no. EN-005; In Vitro). Mycoplasma testing of parental and MDCK-E7 cells was performed using a mycoplasma detection kit for conventional PCR (cat. no. 11-8005; Vector® Gem OneStep; Minerva Biolabs GmbH) according to the manufacturer´s instructions.

Immunofluorescence. Reproductive female tracts containing the vagina, cervix and both uterine horns were removed from the FvB and K14E7 mice treated with or without E_2. The tissue was then immersed in tissue freezing mounting media (cat. no. 14020108926, Tissue Tek; Leica Microsystems GmbH) and incubated at -70˚C for 24 h. Next, 5-7-μm sections were cut using a Leica MC1510 cryostat (Leica Microsystems GmbH) and mounted on pre-cooled (-20˚C) gelatin-coated slides. The slides were then incubated at -70˚C for 24 h. Subsequently, the sections were fixed with 100% ethanol at -20˚C for 20 min and the remaining protocol was performed as previously described (31). Using a confocal microscope (Leica TG5 SP8; Leica Microsystems GmbH) with a x63 objective, images were captured of the squamous multilayered epithelium of the exocervix only, where the basal epithelial cells are the site of infection of HPV in women (32). Immunofluorescence of claudins in parental and MDCK-E7 cells at the TER peak (18 h) following the Ca-switch, was performed following a previously described protocol (31).

The following primary antibodies were used for the immunofluorescence experiments in both mouse cervix and MDCK cells: rabbit antibodies against claudin-1 (cat. no. 51-9000, dilution 1:100) and claudin-10 (cat. no. 38-8400; dilution 1:100) (both Invitrogen; Thermo Fisher Scientific, Inc.). In addition, in MDCK cells the following mouse monoclonal primary antibodies were used: against E7 protein of HPV16 (cat. no. ab30731; dilution 1:100; Abcam), claudin-2 (cat. no. sc-293233; dilution 1:100; Santa Cruz Biotechnology Inc.) and claudin-4 (cat. no. 32-9400; dilution 1:100; Invitrogen; Thermo Fisher Scientific, Inc.). The following secondary antibodies were used: donkey anti-rabbit IgG coupled to Alexa-Fluor 488 (cat. no. A21206; dilution 1:500), donkey anti-mouse coupled to Alexa-Fluor 594 (cat. no. A21203; dilution 1:1,000), or donkey anti-rabbit coupled to Alexa-Fluor 594 (cat. no. A21207; dilution 1:1,000) (all Invitrogen; Thermo Fisher Scientific, Inc.). In parental MDCK and MDCK-E7 cells actin was detected using rhodaminated phalloidin (cat. no. P1951; dilution 1:50; Sigma-Aldrich; Merck KGaA). Slides were mounted with Vectashield with DAPI (cat. no. H1200; Vector Laboratories, Inc; Maravai Life Science).

All the antibodies used reacted with mouse and dog tissues according to the manufacturer's instructions. The two exceptions are the monoclonal antibody against claudin-2 and the anti-claudin-10 polyclonal antibody, in which no details were provided regarding the reactivity with dog tissue. However, the monoclonal antibody against claudin-2, was raised against amino acids 29-80 of the human claudin-2 protein, and a blast sequence analysis revealed a 96% identity and 98% similarity between human and dog claudin-2 (data not shown). The polyclonal antibody against claudin-10 was successfully used in MDCK cells in a previous study (33).

Relative mean fluorescence intensity measurements. The relative mean fluorescence intensity measurements of claudins -1 and -10 in the cervix of the FvB and K14E7 mice treated with or without E_2, and of claudins -1, -2, -4 and -10 in MDCK cells were obtained using ImageJ software (v1.52n, National Institutes of Health) using the freehand function. The integrated density feature of ImageJ was used to record pixel intensities per area. Data were derived from three images of the cervix for all the experimental groups: FvB and K14E7 mice treated with or without E_2 at 2-, 4- and 7-months of age.

Transmission electron microscopy (TEM). The reproductive female tracts containing the vagina, cervix and both uterine horns were removed from 2- and 7-month-old female FvB and transgenic K14E7 mice treated with or without E_2. Subsequently 1-mm width discs from the middle of the exocervix were excised. Samples were fixed at room temperature with 2.5% (v/v) glutaraldehyde in 0.1 M sodium cacodylate buffer, pH 7.2, for 60 min. Samples were then treated at room temperature for 60 min with a solution of 1% (w/v) osmium tetroxide in 0.1 M sodium cacodylate buffer, containing 0.5 mg/ml ruthenium red. Following dehydration with increasing concentrations of ethanol and propylene oxide, samples were embedded in Polybed epoxy resins and polymerized at 60˚C for 24 h. Thin sections (60-nm) were stained at room temperature for 20 min with uranyl acetate and subsequently for 2 min with lead citrate prior to examination at a magnification of x20,000, using a Jeol JEM-1011 transmission electron microscope.

The permeability of the TJ present in the superficial cells of the multi-stratified epithelium of the cervix of mice was evaluated using the paracellular pathway marker ruthenium red, as previously reported (34,35). Thus, if the ruthenium red stain only highlighted the apical surface of the superficial cells in the cervix, this indicated that passage through the paracellular pathway was blocked due to TJ sealing. Instead, if the staining was present along the paracellular pathway, below the TJ region, in the superficial cells of cervix, the TJ was opened.

Stable transfection of MDCK cells with E7 oncoprotein. MDCK cells at 70% confluence were transfected with 3 μg of pcDNA3E7 plasmid as previously described (36) using Lipofectamine® 2000 (cat. no. 11668019; Invitrogen; Thermo Fisher Scientific, Inc.) according to the manufacturer's instructions. To generate the stable MDCK-E7 clones, the cells were harvested using trypsinization and plated at a density of $3x10^4$ cells/cm^2 on 100-mm culture dishes with DMEM containing 800 μg/ml geneticin (G418; cat. no. 11811-031; Gibco; Thermo Fisher Scientific, Inc.), 48 h following transfection. Resistant clones were selected and re-cloned manually using the cloning ring technique, after 2-3 weeks (37). Stable colonies were maintained in the presence of 200 μg/ml G418.

PCR amplification of E7. Total RNA was extracted from parental and E7 MDCK cells using TRIzol® reagent (cat. no. 15596026; Invitrogen; Thermo Fisher Scientific, Inc.) following the manufacturer's instructions. RNA purity and concentration were measured using a Nanodrop™ ND-8000 spectrophotometer (cat. no. ND-8000-GL; Thermo Fisher Scientific, Inc.) and its integrity was determined using electrophoresis in 1% agarose gels, by resolving the 28S and 18S ribosomal RNA bands. cDNA was synthesized from RNA using SuperScript One-Step reverse transcription (RT)-PCR with platinum Taq DNA polymerase (cat. no. 10928042; Invitrogen; Thermo Fisher Scientific, Inc.), following the manufacturer's instructions and a Biometra GmbH Professional Basic Gradient thermocycler (cat. no. 070-601; Analytik, Jena US LLC). The PCR for HPV16 E7 was performed in a final 25 μl volume containing: 1 μg template RNA, 0.2 μM forward and reverse primers for HPV16 E7, 1U RT/Platinum Taq mix, 1.2 mM $MgCl_2$ and 200 μM dNTPs. The primers were designed according to E7 gene sequence obtained from GenBank (accession no. AF125673; www.ncbi.nlm.nih.gov/nuccore/4927719); and had the following sequence: Forward, 5'-CTCAGAGGAGGAGGATGAAATAG-3'; and reverse, 5'-CTGAGAACAGATGGGGCACAC-3'. cDNA synthesis was performed at 50˚C for 30 min and at 94˚C for 2 min. The following thermocycling conditions were used: Initial denaturation at 94˚C for 15 sec followed by 25 cycles of 94˚C for 1 min, 60˚C for 30 sec and 72˚C for 1 min. The PCR products were separated on 1.5% agarose gels and images were obtained following ethidium bromide staining. The expected amplicon size was 196 bp.

Western blot analysis. Western blots of lysates from the cervix of FvB and K14E7 mice treated with or without E_2, of 2-, 4- and 7-months of age and of parental and MDCK-E7 cells at the TER peak (18 h) following the Ca-switch, was performed following standard procedures, as previously described (31). The following primary antibodies were used: rabbit polyclonal anti-claudin-1 (cat. no. 51-9000; dilution 1:500; Invitrogen; Thermo Fisher Scientific, Inc.), claudin-10 (cat. no. 38-8400; dilution, 1:500; Invitrogen, Thermo Fisher Scientific, Inc.) and GAPDH (cat. no. RPCA-GAPDH; dilution 1:40,000; Encor Biotechnology Inc.). In addition, for MDCK cells the following primary antibodies were used: rabbit polyclonal anti-claudin-2 (cat. no. 51-6100, dilution 1:1,000; Invitrogen; Thermo Fisher Scientific, Inc.), and claudin-4 (cat. no. 36-4800; dilution 1:500; Invitrogen; Thermo Fisher Scientific, Inc.), and a mouse monoclonal against actin (generated and provided by Dr Manuel Hernández, Department of Cell Biology, Center for Research and Advanced Studies, Mexico city, Mexico). The following secondary antibodies were used: goat anti-rabbit IgG conjugated to horseradish peroxidase (HRP; cat. no. 6111620; dilution 1:20,000; Invitrogen; Thermo Fisher Scientific, Inc.), or goat anti-mouse IgG conjugated to HRP (cat. no. 626520; dilution 1:10,000; Invitrogen; Thermo Fisher Scientific, Inc.). The proteins were visualized using a Immobilon chemiluminescence detection (cat. no. WVKLS 0500; EMD Millipore).

All the antibodies used react with mouse and dog tissues according the manufacturer's instructions. The only exception was the polyclonal anti-claudin-10 antibody, in which there was no information regarding its reactivity on dog tissue. However, this antibody was successfully used in MDCK cells in a previous study (33).

TER. Parental and MDCK-E7 cells were cultured at a density of $1.2x10^5$ cells/cm^2 on 1.12 cm^2 Transwell polyester membrane clear inserts (cat. no. 3460; pore size 0.4 μm; Corning Inc.). Confluent monolayers of control and MDCK-E7 cells were transferred from normal calcium (NC; 1.8 mM Ca^{2+}; cat. no. 12800-082; Gibco; Thermo Fisher Scientific Inc.) containing media to low calcium (LC; 1-5 μM Ca^{2+}; cat. no. D9800-10.10; United States Biological) media for 22 h. Subsequently, the monolayers with no TER (time 0) were changed to NC media (Ca-switch) to trigger TJ formation and TER development. TER was measured continuously and without interruptions for 63 h from each insert using an automated cell monitoring system (cellZscope version CZS0101909; nanoAnalytics GmbH). TER values were obtained using the CellZscope software (version 2.2.0.16827; nanoAnalytics GmbH). Statistical analysis using the Student's t-test was used to investigate the TER observed in parental and MDCK-E7 cells at the peak of resistance obtained at 18 h.

Cell migration assay in a 3D matrix. MDCK and MDCK-E7 cells were plated at a density of $2.4x10^5$ cells/cm^2 on 12-well inserts containing Alvetex® 3-dimentional polystyrene scaffold (cat. no. AVP005-12; Reinnervate Ltd.) precoated at room temperature for 2 h with basement membrane matrix BD Matrigel™ (cat. no. 356230, BD Biosciences) at a concentration of 0.8 mg/ml, according to the manufacturer's instructions. Every second day DMEM media with 10% fetal calf serum was changed from the upper and lower chambers. The migration of MDCK and MDCK-E7 cells was evaluated using confocal immunofluorescence in 10-day-old cultures where the cells were stained with rhodaminated phalloidin (cat. no. P1951; Sigma-Aldrich; Merck KGaA) for 2 h at room temperature, and mounted with Vectashield (cat. no. H-1200; Vector Laboratories; Maravai LifeSciences) antifade mounting medium containing DAPI, which fluoresces blue when bound to DNA. Images were captured using a confocal microscope (Leica TG5 SP8) with a x63 objective in the z plane using LAS AF X software (version 3.0; Leica Microsystems GmbH). A depth coded z series image was generated from red to blue, where warmer colors (red) correspond to cells that have not migrated to the bottom of the scaffold and are still located on the surface, whereas colder colors (blue) represent the cells that have migrated deeper in the scaffold.

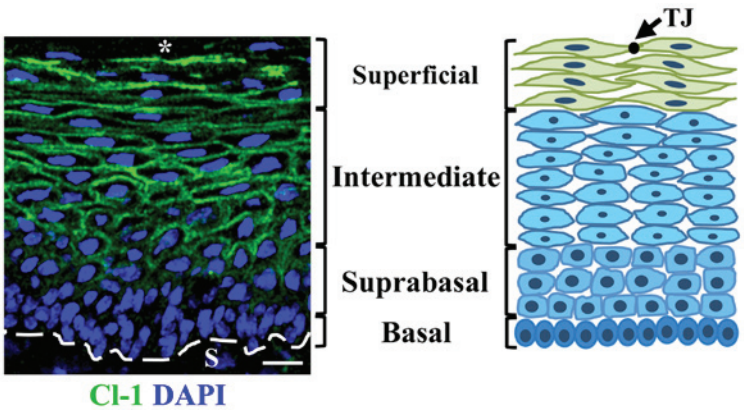

Figure 1. Immunofluorescence of Cl-1 in the cervix with a corresponding diagram illustrating the different layers of the multi-stratified tissue. Comparison of a frozen section of the cervix from a 2-month-old FvB mouse, without E_2 treatment, incubated with anti-Cl-1 antibody (left panel), with a schematic representation of the multi-stratified organization of the cervix (right panel). The tight junction (TJ) is represented as a black dot in the schematic diagram showing connecting, neighboring cells in the upper cell layer of the cervix. Left panel, the nuclei were stained with DAPI and the dashed white line represents the border between the epithelial basal cell layer and the stroma. Scale bar, 15 μm. *lumen; S, stroma; Cl, claudin; TJ, tight junction.

Atomic force microscopy. The nanomechanical properties of the apical surface of parental and MDCK-E7 cells present as either isolated cells or as islands of cells was analyzed using Atomic force microscopy. The cells were plated at a density of $1.5x10^4$ cells/cm^2 on ultra flat silicon wafers placed in 12-well plates and incubated at 36.5˚C in a humidified incubator with 5% CO_2 with DMEM (cat. no. 12800-082; Gibco; Thermo Fisher Scientific, Inc.) supplemented with 10% fetal bovine serum (cat. no. S1650-500; Biowest). The cells were fixed for 10 min with 4% paraformaldehyde at room temperature, after 8 h. All measurements were performed using a Solver Next Atomic Force Microscope from NT-MDT Spectrum Instruments. Elastic Modulus were measured based on the deviation force lateral (DFL) curves (displacement of cantilever vs. distance). A cantilever contact type CSG10, was used with a curvature radius of 10 nm. Scanning conditions for the cells were as follows: A ramp size set to 80 μm for islets and 50 μm for isolated cells, with a gain of 0.18 and a rate of 0.3 Hz with 256 points. Experimental data were analyzed using the Image Analysis Software (v3.5; NT-MDT Spectrum Instruments) to determine Young´s modulus in kPa.

Statistical analysis. The statistical analysis between multiple groups in different experimental conditions (Figs. 2B and C, and 4B and C) was performed using three-way ANOVA followed by Tukey's post hoc test. The statistical analysis between 2 groups (Figs. 3B, 5B, 8A, C and D, and 9B) was performed with Student's t-test. Statistical analysis was performed using Prism GraphPad v6 (GraphPad Software Inc.). Data are presented as mean ± standard deviation. Number of repeats are indicated in the legend of each figure.

Results

Transgenic K14E7 mice treated with E_2 develop invasive cancer with a reduced expression of claudin-1. The expression of claudin-1 in the multi-stratified epithelium of the cervix of control FvB and transgenic K14E7 mice treated with or without E_2 was investigated. In control FvB mice, at 2 months of age, claudin-1 is present at the border of cells from the suprabasal region up to the most superficial cell layer facing the cervix lumen where it is expressed with higher intensity, while no claudin-1 expression is present in the basal cell layer (Fig. 1). In mice at 4- and 7-months of age the expression of claudin-1 was present at the basal cell layer augments and neither, treatment of FvB mice with E_2 nor the expression of E7 in the transgenic K14E7 mice changed this pattern of expression (Figs. 2A and S1-4). Quantitative analysis revealed no change in claudin-1 immunofluorescence intensity in the cervix between FvB mice at 2-, 4-, and 7-months of age with or without E_2 treatment (Fig. 2B). In 2-month-old K14E7 mice without E_2 treatment, there was an increase in claudin-1 expression compared with that in FvB mice, and FvB and K14E7 mice treated with E_2 (Fig. 2B). Western blot analysis of claudin-1 in the cervix of the aforementioned mice confirmed the increase in claudin-1 protein expression in 2-month-old K14E7 mice without treatment with E_2 compared with that in 4- and 7-month-old K14E7 mice without E_2 treatment, and in 2-month-old FvB mice without E_2 and K14E7 mice with E_2 (Fig. 2C).

Treatment of transgenic K14E7 mice with E_2 induces the appearance of papillomas which develop progressively with age. In carcinomas that project into the cervical stroma of 7-month-old mice, the expression of claudin-1 was reduced compared with that in the rest of the cervix (Fig. 3A and B).

Claudin-10 localizes at an earlier age in the upper layer of the cervix in FvB mice treated with E_2 and K14E7 mice treated with or without E_2. Subsequently, the expression of claudin-10 in the cervix of control FvB and transgenic K14E7 mice treated with or without E_2 was investigated (Figs. S5-8). Claudin-10 was expressed in a diffuse cytoplasmic pattern, from the basal to the uppermost layers of the cervix in FvB mice without E_2 treatment at 2- and 4-months of age (Fig. 4A-a and -e); however, it was found to be expressed at the border of cells in the superficial cell layers in 7-month-old mice (Fig. 4A-i). The expression of claudin-10 in FvB mice treated with E_2 and in K14E7 mice treated with and without E_2 was located in the border of cells in the in the upper cell layers

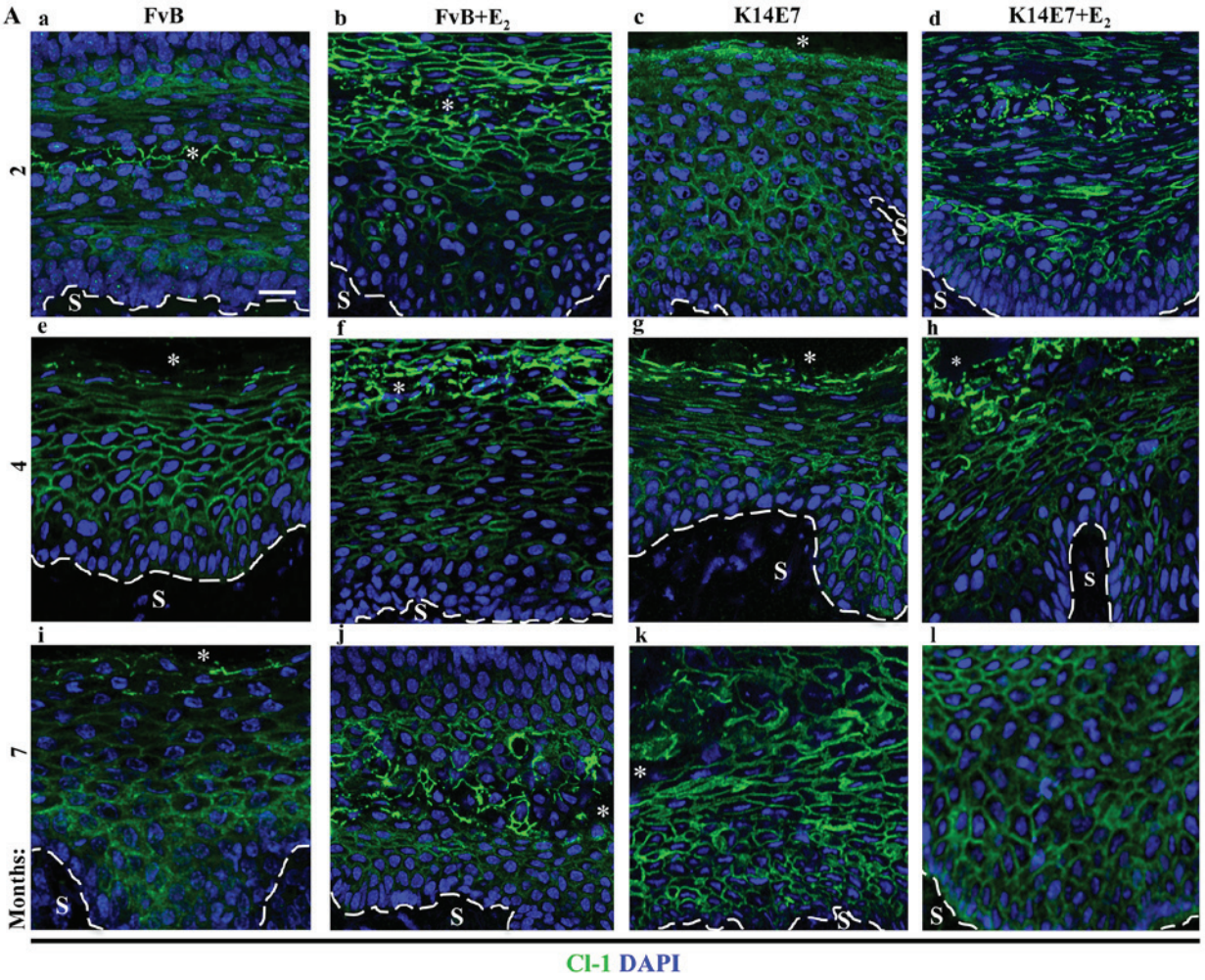

Figure 2. Oncogenic protein E7 augments the expression of Cl-1 in the cervix of 2-month-old mice, while treatment with E_2 abolishes this effect. Expression of Cl-1 from frozen sections of the cervix obtained from (A-a-d) 2-, (A-e-h) 4- or (Ai-l) 7-month-old (A-a, -e and -i) control FvB without E_2 or (A-b, -f and -j) with E_2 and transgenic K14E7 mice, treated (A-d, -h and -l) with E_2 or (A-c, -g and -k) without E_2, using immunofluorescence. Nuclei were stained with DAPI. Dashed white line indicates the border between the epithelial basal cell layer and the S. *Cervical lumen. Scale bar, 20 μm.

from the second month of life (Fig. 4A--b-d, -f-h, and -j-l). Quantitative analysis revealed a significant higher fluorescence intensity of claudin-10 in the cervix of FvB mice treated with E_2 at 2-months of age compared with that in mice at 4- and 7-months of age, and these values were similar to those in K14E7 mice treated with or without E_2 at 2-, 4- and 7-months of age (Fig. 4B). In addition, the quantitative fluorescence intensity of claudin-10 in 2-month-old FvB mice was higher compared with that observed in 7-month-old K14E7 mice without E_2 treatment and in 2- and 7-month-old K14E7 mice treated with E_2 (Fig. 4B). The western blot analysis of claudin-10 protein expression in the cervix of the aforementioned mice decreased in a time-dependent manner in both FvB and K14E7 mice treated with or without E_2, whereas in K14E7 mice treated with E_2 the level of claudin-10 at 4- and 7-month of age was lower compared with that in K14E7 mice without E_2 treatment, which were 2-months old (Fig. 4C).

Furthermore, in 7-month-old transgenic K14E7 mice treated with E_2, the papillomas which can invade the stroma showed a low expression levels of claudin-10, similar to that observed in the lower layers of the rest of the cervix (Fig. 5A and B).

Opening of TJs at the cervix superficial cell layer is induced by E_2 or E7. To determine if the changes observed in the expression of claudins -1 and -10 were accompanied with an increase in the paracellular permeability of the cervix, further analysis was performed. Fig. 6A shows a semi-thin section of the cervix in a 2-month-old FvB mouse without E_2 treatment, where the ruthenium red stain was found to be located in the lumen, which was in contact with the apical surface of the superficial layer of cells in the multistratified epithelium. Subsequently, using transmission electron microscopy, the thin sections found in the cervix of 2-month-old FvB mice, without E_2 treatment, were impermeable to the paracellular electrodense marker, ruthenium red, which was found to be maintained in FvB mice at 7-months-old (Fig. 6B-a and -e). In contrast, in FvB mice at 2- and 7-months-old treated with E_2, 29 and 36% of TJ were permeable to ruthenium red, respectively (Fig. 6B-b and -f). There percentage permeability in K14E7 mice treated without E_2 was 67 and 55%, at 2- and 7-months of age, respectively (Fig. 6B-c and -g), which was similar to that found in K14E7 mice treated with E_2 (Fig. 6B-d and -h).

Therefore, it was concluded that the increase in TJ permeability in the cervix of FvB mice treated with E_2 occurs at

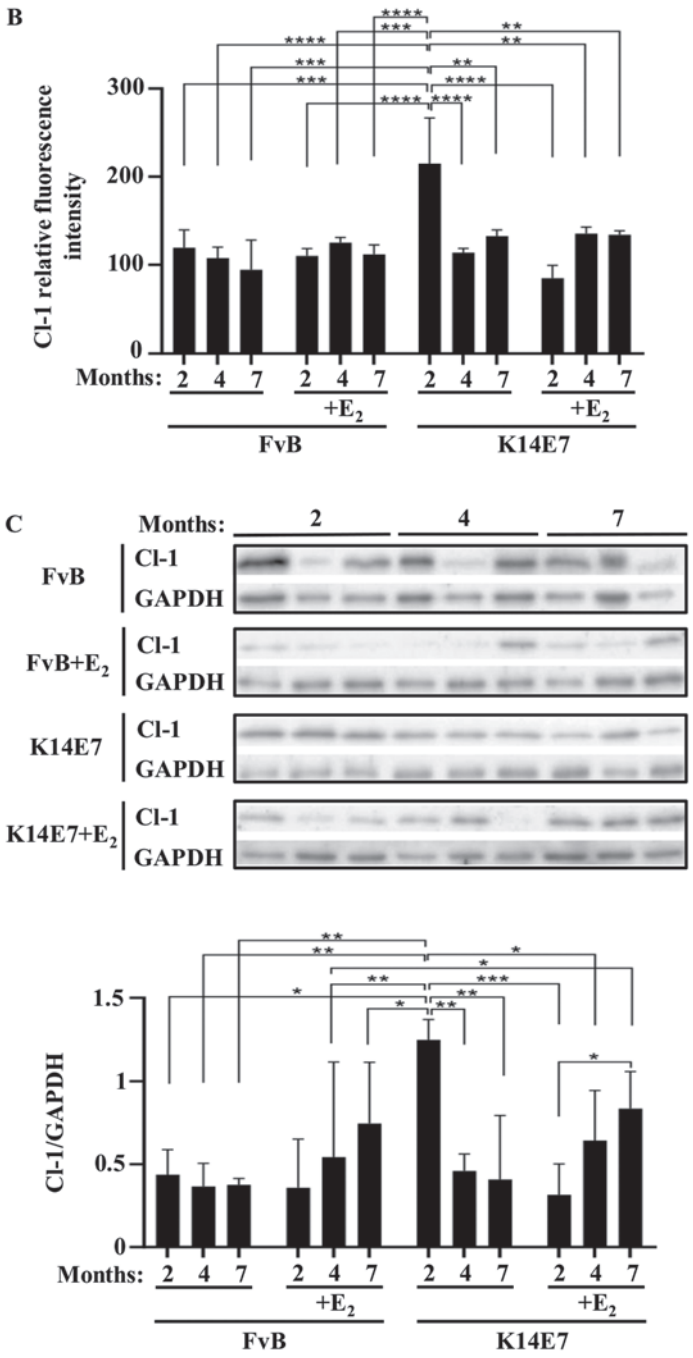

Figure 2. Continued. (B) Quantitative analysis of the mean fluorescence intensity of Cl-1 observed in frozen sections of the cervix obtained from 2-, 4- or 7-month-old control FvB and transgenic K14E7 mice, treated with or without E_2. Results obtained from three independent images from each experimental group. Statistical analysis performed using three-way ANOVA followed by Tukey's post hoc test. Data are presented as mean ± standard deviation. **P<0.01, ***P<0.001, ****P<0.001. (C) Representative western blot of Cl-1 in cervix lysates obtained from 2-, 4- or 7-month-old control FvB and transgenic K14E7 mice, treated with or without E_2 (upper panel). Densitometry analysis from at least three independent experiments (lower panel). Statistical analysis was performed using three-way ANOVA followed by Tukey's post hoc test. Data are presented as mean ± standard deviation. *P<0.05, **P<0.01, ***P<0.001. S, Stroma; Cl, claudin; E_2, 17β-estradiol.

the same age (2-months old) when a change in the expression pattern of claudin-10 was observed.

The stable expression of E7 alters the monolayer architecture of epithelial MDCK cells. To improve the understanding of E7 on epithelial cell transformation, a stable transfection of HPV16 E7 oncoprotein in epithelial MDCK cells was created, which is a cell line characterized for exhibiting well developed TJs (38), and has frequently been used to investigate the effect of viruses and viral proteins on TJs (39-43). Fig. 7A revealed that E7 was expressed in clones 1 and 5 of MDCK-E7 cells but not in parental MDCK cells using RT-PCR. As the expression of E7 was the same in all clones, clone 5 was selected to be used in further experimentation. Fig. 7B shows that the E7 protein is expressed in a diffuse manner in MDCK-E7 cells, while there is no expression in parental MDCK cells, using immunofluorescence. Light microscopy images of semi-thin sections reveal that MDCK-E7 cells grow in an abnormal

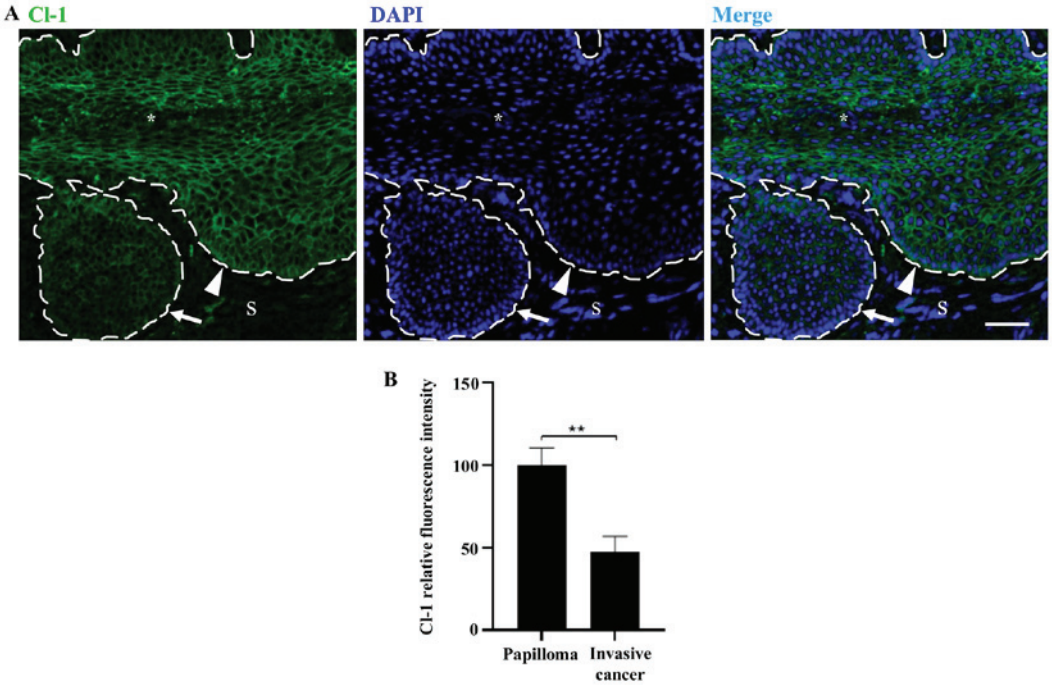

Figure 3. Expression of Cl-1 is reduced compared with that in the rest of the cervix, in invasive cancer. (A) Expression of Cl-1 in frozen sections of cervix from a 7-month-old transgenic K14E7 mouse treated with 17β-estradiol using immunofluorescence. Nuclei were stained with DAPI. The dashed white line indicates the border between the epithelial basal cell layer and the S. *Cervical lumen. Scale bar, 50 μm. The arrow indicates invasive cancer and the arrowhead indicates papilloma. (B) Comparison of mean fluorescence intensity of claudin-1 in invading papillomas compared with that in the rest of the cervix. Data obtained from three independent images. Statistical analysis was performed using the Student's t-test. Data are presented as the mean ± standard deviation. **P<0.01. S, stroma; Cl, claudin.

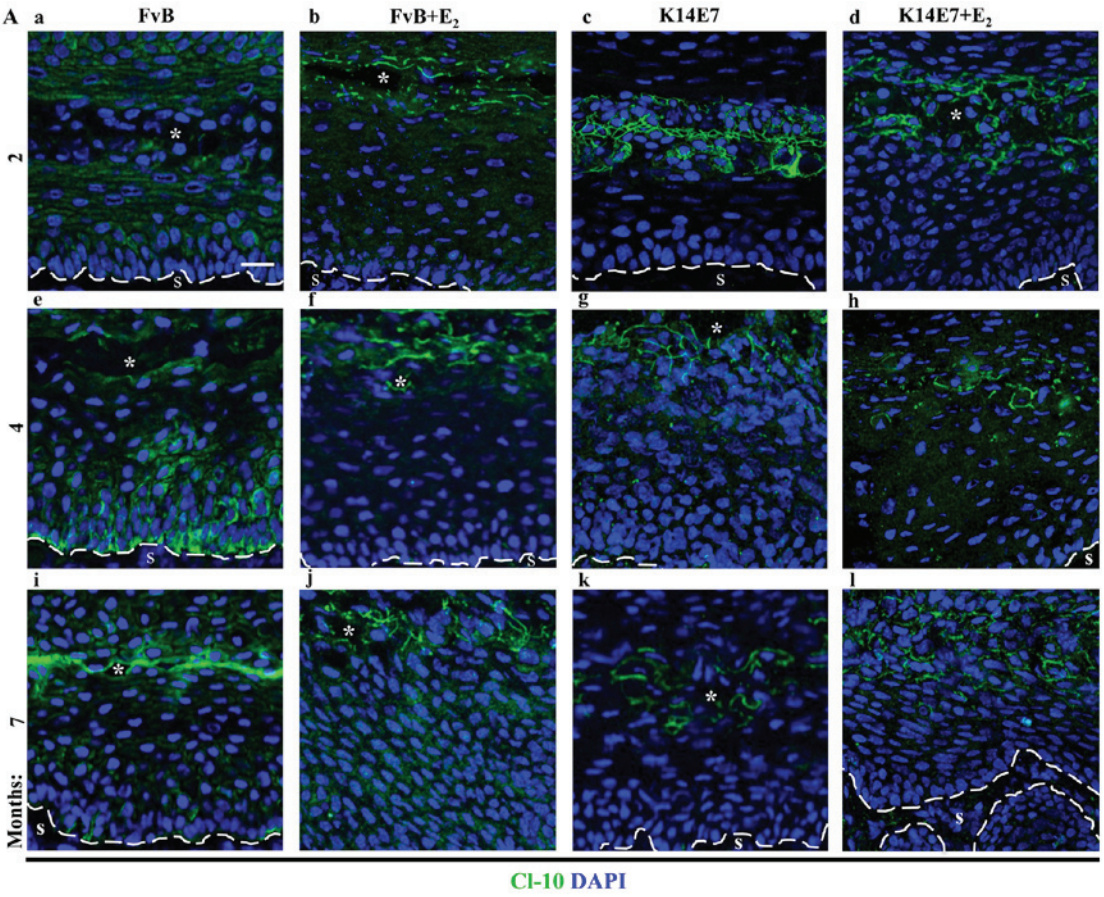

Figure 4. Treatment of FvB and K14E7 mice with and without E_2 increases the expression of Cl-10 at the border of cells in the superficial layer of the cervix. Expression of Cl-10 in frozen sections of the cervix obtained from (A-a-d) 2-, (A-e-h) 4- or (Ai-l) 7-month-old control FvB (A-a, -e and -i) without E_2 or (A-b, -f, and -j) with E_2 and transgenic K14E7 mice, treated (A-d, -h and -l) with E_2 or (A-c, -g and -k) without E_2, using immunofluorescence. Nuclei were stained with DAPI. Scale bar, 20 μm. The dashed white line indicates the border between the epithelial basal cell layer and the S. *Cervical lumen.

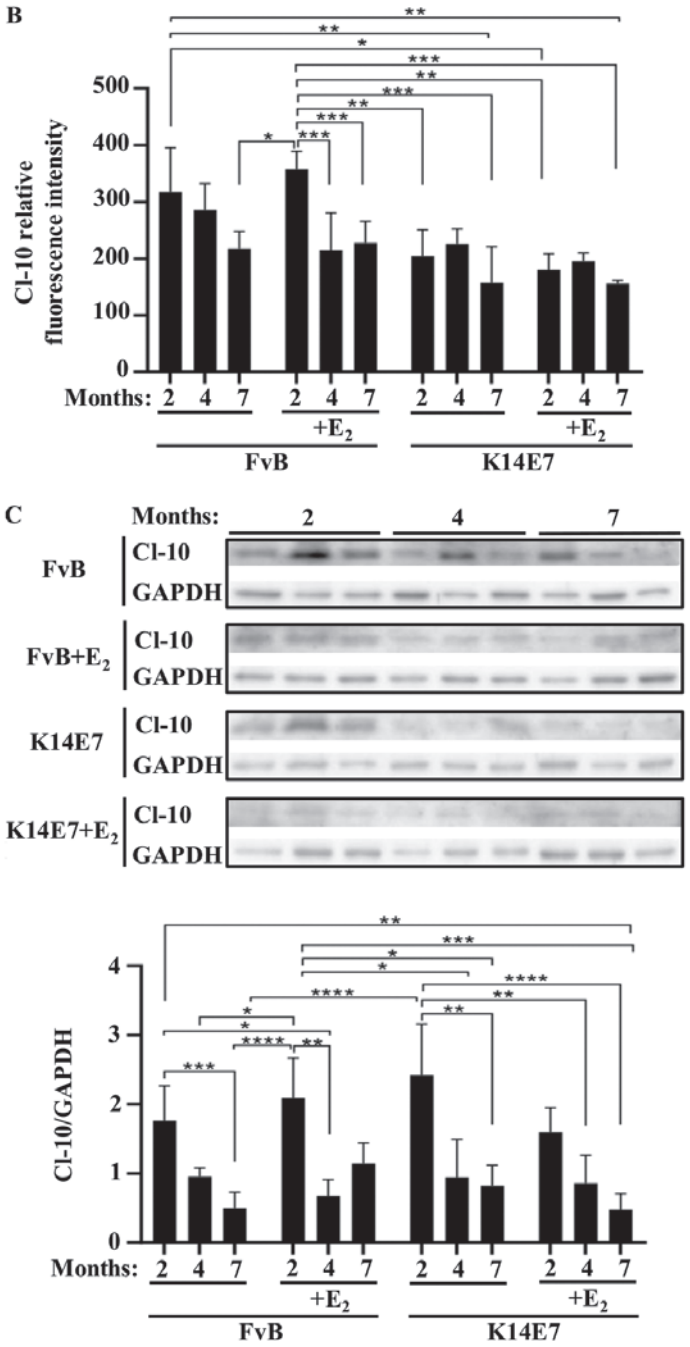

Figure 4. Continued. (B) Quantitative analysis of the mean fluorescence intensity of Cl-10 from frozen sections of the cervix obtained from 2-, 4- or 7-month-old control FvB and transgenic K14E7 mice, treated with or without E_2. Results obtained from three independent images from each experimental group. Statistical analysis was performed using three-way ANOVA followed by Tukey's post hoc test. Data are presented as the mean ± standard deviation. *P<0.05, **P<0.01, ***P<0.001. (C) Representative western blot of Cl-10 in cervix lysates obtained from 2-, 4- or 7-month-old control FvB and transgenic K14E7 mice, treated with or without E_2 (upper panel). Densitometry analysis from at least three independent experiments (lower panel). Statistical analysis was performed using three-way ANOVA followed by Tukey's post hoc test. Data are presented as the mean ± standard deviation. *P<0.05, **P<0.01, ***P<0.001, ****P<0.0001. E_2, 17β-estradiol; S, stroma; Cl, claudin.

manner characterized by the presence of some cells growing on top of one another and by the widening of intercellular spaces (Fig. 7C). These observations were further confirmed by TEM (Fig. 7D).

E7 induces the development of an acute peak of TER in MDCK monolayers and changes the expression pattern of claudins-1 and -10. Subsequently, if the development of TER was altered by the expression of E7 in MDCK cells was investigated and the Ca-switch procedure to trigger TJ formation and TER development was used. Fig. 8A shows that MDCK-E7 cells reached a much higher peak of TER compared with that in the control cells. However, at 40 h following the Ca-switch, when the TER stabilizes in both cell lines, both experimental groups display similar TER values. Next, the expression of claudins-1 and -10 at the TER peak (18 h) following the Ca-switch was investigated. In addition, the expression levels of claudins-2 and -4 were also investigated, as the former forms paracellular

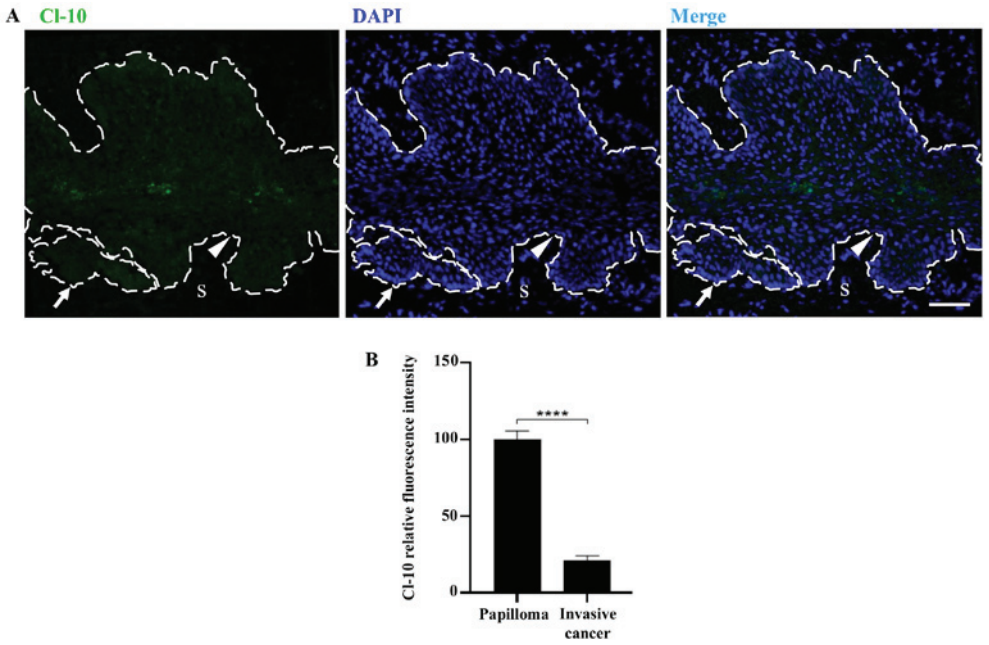

Figure 5. Expression of Cl-10 is low and similar to that present in the lower layers of the cervix, in invasive cancer. (A) Expression of Cl-10 in frozen sections of cervix from 7-month-old transgenic K14E7 mice treated with 17β-estradiol using immunofluorescence. Nuclei were stained with DAPI. The dashed white line indicates the border between the epithelial basal cell layer and the S. Scale bar, 50 μm. The arrow indicates invasive cancer and the arrowhead indicates papilloma. (B) Comparison of mean fluorescence intensity of Cl-10 in invading papillomas compared with that in lower layers of cells in the cervix. Data obtained from three independent images. Statistical analysis was performed using the Student's t-test. Data are presented as the mean ± standard deviation. Nuclei were stained with DAPI. ****P<0.0001. S, stroma; Cl, claudin.

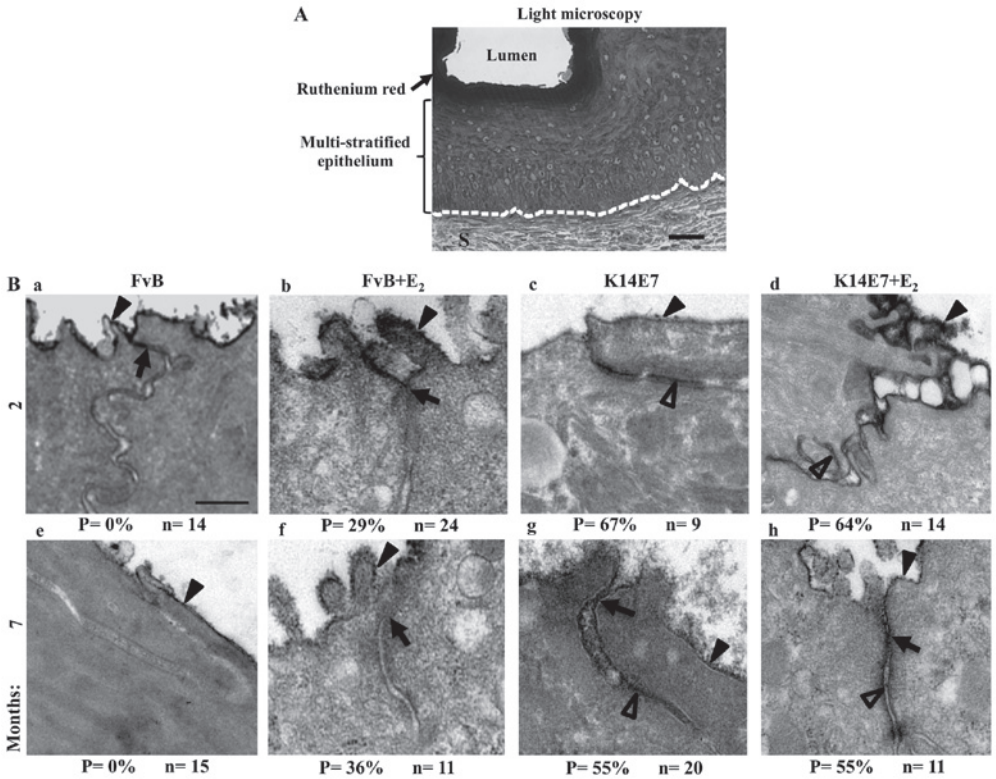

Figure 6. Treatment with E_2 induces opening of TJs in the cervix of transgenic K14E7 mice. (A) Semi-thin section of the cervix from a 2-month-old FvB mouse stained with ruthenium red. The dashed white line indicates the border between the epithelial basal cell layer and the S. Scale bar, 25 μm. Transmission electron microscopy of thin sections from ruthenium red stained cervix from (B-a-d) 2- and (B-e-h) 7-month-old FvB mice (B-b and -f) with E_2 or (B-a and -e) without E_2, and transgenic K14E7 mice, treated (B-d and -h) with E_2 or (B-c and -g) without E_2. In 2- and 7-month-old FvB mice the ruthenium red stain highlighted the apical surface of the superficial cells in the multi-stratified epithelium of the cervix, while negative staining was found in the paracellular pathway, below the TJ region, in this layer of cells. In FvB mice treated with E_2 and in K14E7 mice treated with or without E_2, the ruthenium red stain highlighted a percentage of the cells along the paracellular route of the superficial layer of cells in the cervix. Scale bar, 250 nm. Black arrowheads indicate ruthenium red staining in the apical surface. The arrows indicate TJs and the empty arrowheads indicate ruthenium red staining in the paracellular pathway between adjacent cells. P, permeable TJs; n, number of observations; TJ, tight junctions; E_2, 17β-estradiol.

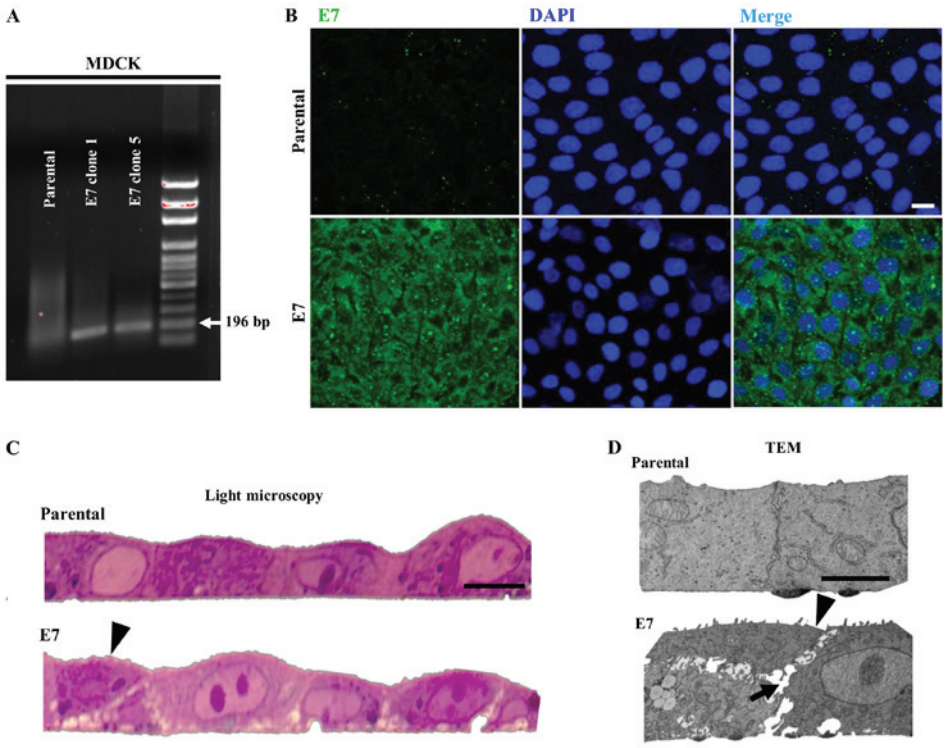

Figure 7. E7 from HPV16 alters the cytoarchitecture of epithelial monolayers. (A) E7 was expressed in MDCK-E7 clones stably transfected with E7 from HPV16, but not in parental MDCK cells. (B) E7 protein displays a speckled staining in MDCK-E7 cells using immunofluorescence. DAPI was used for nuclear staining. Scales bar, 10 μm. (C) Light microscopy images of semi-thin sections of MDCK-E7 and parental MDCK cells. Arrowhead indicates cells growing on top of one another. Scale bar, 10 μm. (D) TEM of thin sections of MDCK-E7 and parental MDCK cells. Arrowhead indicates the cells growing on top of one another; arrows indicates the widened intercellular space. Upper bar, 500 nm; lower bar, 2.5 μm. MDCK, Madin-Darby Canine Kidney; TEM, transmission electron microscopy; HPV, human papillomavirus.

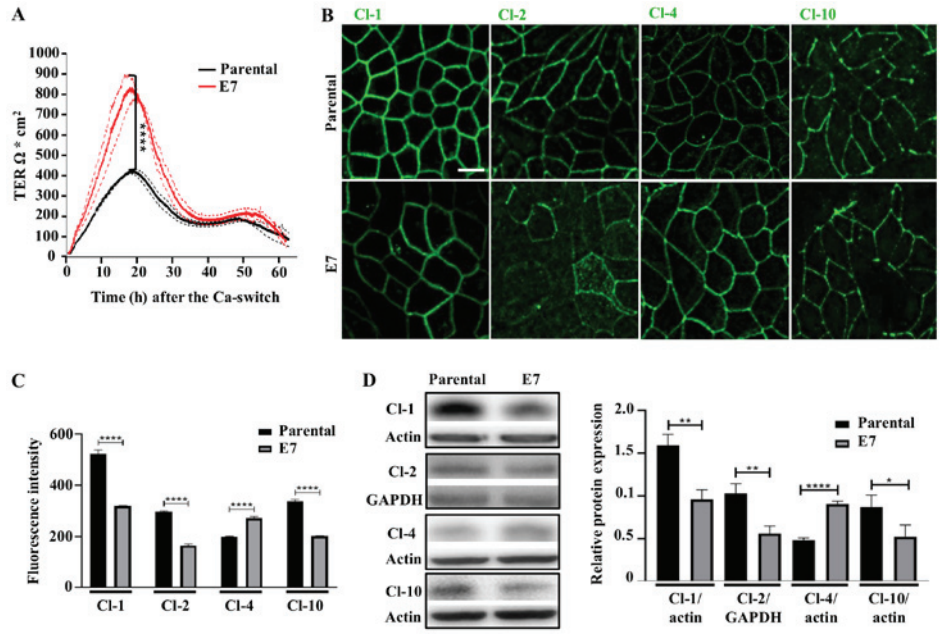

Figure 8. Stable expression of E7 in MDCK monolayers induces the development of a higher peak of TER and changes the expression of claudins. (A) Parental MDCK and MDCK-E7 monolayers plated in Transwell inserts were subjected to a Ca-switch and the development of TER was measured using the automated cell monitoring system, cellZscope. Data are presented the mean ± SD from three independent monolayers per condition plated on Transwell inserts. Statistical analysis was performed at the 18 h with Student's t-test. ****P<0.0001. (B) Immunofluorescence detection of Cl-1, -2, -4 and -10 at the peak of TER (18 h) in parental and MDCK-E7 monolayers. Representative images from three independent experiments. Scale bar, 10 μm. (C) Mean fluorescence intensity measurements of Cl-1, -2, -4 and -10 performed at the peak of TER (18 h) in parental and MDCK-E7 monolayers. Data derived from three independent images from each condition and from three independent experiments. Statistical analysis was performed using Student's t-test. Data are presented as the mean ± standard deviation. ****P<0.0001. (D) Western blot analysis of Cl-1, -2, -4 and -10 at the peak of TER (18 h) in parental and MDCK-E7 monolayers. Representative western blots of at least three independent experiments (left panel) and the densitometry analysis (right panel). Statistical analysis was performed using Student's t-test. Data are presented as the mean ± standard deviation. *P<0.05, **P<0.01, ****P<0.0001. Ca, calcium; Cl, claudin; TER, transepithelial electrical resistance; MDCK, Madin-Darby Canine Kidney; MDCK-E7, MDCK cells transfected with E7 from HPV; HPV, human papillomavirus.

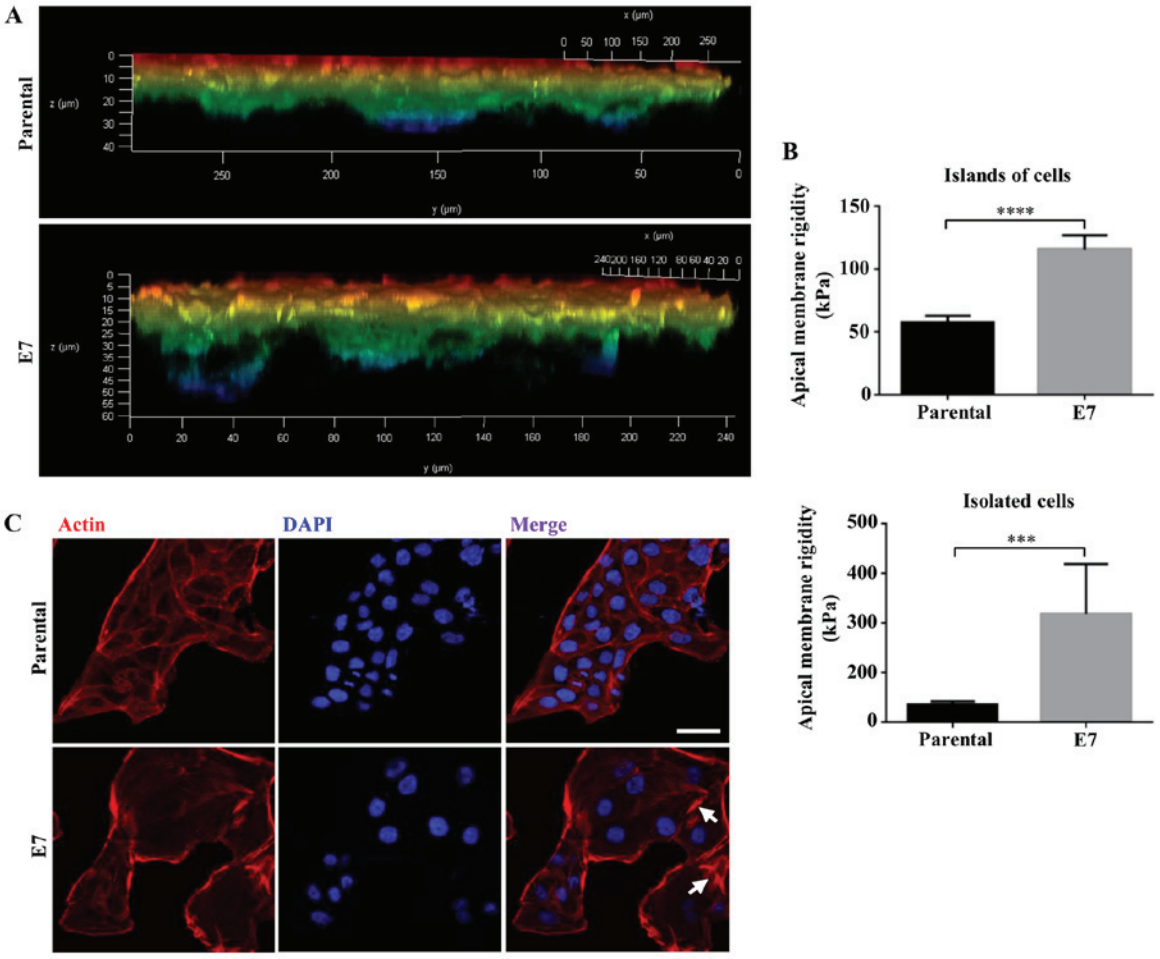

Figure 9. MDCK-E7 cells migrate further through a 3D scaffold, have a stiffer apical surface and display more stress fibers compared with that in control MDCK cells. (A) MDCK and MDCK-E7 cells were seeded on top of 12-well insert containing Alvetex® Scaffold precoated with Matrigel™. Cells were stained with rhodaminated phalloidin following 10 days of culture. Images were captured using a confocal microscope and data analyzed using the Leica LAS AF X software (v3.0), in which a z series image was generated, with a depth color code from red to blue where warmer colors correspond to cells closest to the surface of the scaffold and colder colors to cells that have migrated towards the bottom of the scaffold. Results derived from two independent experiments. (B) Apical membrane rigidity measures were performed using Atomic Force Microscopy in parental and MDCK-E7 cells present as isolated cells or in islets. Statistical analysis was performed using Student's t-test. Data are presented as the mean ± standard deviation. ***P<0.001, ****P<0.0001. (C) The expression of stress fibers (arrows) was higher in MDCK-E7 compared with that in control MDCK cells. MDCK and MDCK-E7 cells were treated with rhodaminated-phalloidin and DAPI, to stain the stress fibers and nuclei, respectively. Scale bar, 30 μm. MDCK, Madin-Darby Canine Kidney; MDCK-E7, MDCK cells transfected with E7 from HPV; HPV, human papillomavirus.

cationic pores (44,45) which increases TJ permeability (46) and decreases TER (47), while the latter exerts the opposite effect, functioning as a cationic barrier (48) or an anionic pore (49). Using immunofluorescence, the expression of claudins-1, and -10 was found to be reduced, while that of claudin-2 was reduced at the cell borders and appeared in a diffuse pattern in the cytoplasm at the peak of TER in MDCK-E7 cells compared with that in parental cells. On the other hand, claudin-4 expression was increased (Fig. 8B and C). These results were further confirmed using western blot analysis (Fig. 8D).

Taken together, the results suggest that the higher peak of TER found in MDCK-E7 cells compared with that in parental monolayers, was due to an altered expression of claudins.

E7 enhances the migrate ability of MDCK cells through a 3D matrix and induces cell stiffening and stress fiber formation. Next, if the presence of E7 induced the migration of MDCK cells was investigated, as this characteristic is important for cancerous cells to invade the underlying stroma and metastasize. A 3D *in vitro* model was used, as it replicates the tissue organization compared with that in 2D models (50). MDCK and MDCK-E7 cells were plated on top of a Matrigel® coated Alvetex®Scaffold, which is a porous and inert polystyrene platform with large voids that create 3D spaces where cells can grow. Fig. 9A shows that MDCK cells migrated through the scaffold between 20 and 30 μm, whereas MDCK-E7 cells migrated to a distance of 50 μm, thus revealing that E7 enhanced the ability of MDCK cells to migrate.

It has been previously shown that cells undergo a stiffening stage prior to acquiring malignant features (51). Therefore, the apical surface elastic Young's module in parental and MDCK-E7 cells was measured using standard nanoindentation force microscopy. The experimental data are supported by their theoretical analysis, which is based on the description of the tip-sample interactions using the Euler-Bernoulli equation (www.efunda.com/formulae/solid_mechanics/beams/theory.cfm) and the asymptotic solutions of the oscillatory tip behavior during its interaction with the sample. Fig. 9B shows

the rigidity of the apical surface of MDCK-E7 increases compared with that in parental cells by 5.64- and 1.99-fold in isolated and in cell islands, respectively. As stiffening is characterized by the accumulation of stress fibers (51), if E7 promoted the expression of stress fibers in MDCK cells was investigated. Fig. 9C shows a proliferation of stress fibers in MDCK-E7 compared with that in control MDCK cells.

Taken together, these results indicate that the E7 oncoprotein promotes cell stiffening and invasion.

Discussion

In the present study a previously characterized transgenic mouse containing the hK14HPV16E7 transgene, where the expression of E7 oncoprotein from HR-HPV16 is regulated by the promoter for human keratin 14 (hK14) (52) was used. The activity of this promoter is restricted to the basal cell layer of multi-stratified epithelia, to guarantee that the expression of E7 is directed to the cell types where HPV infection is targeted. K14E7 transgenic mice display several characteristic phenotypes, including wrinkled skin, thickened ears and loss of hair in adults, and develop skin tumors, which begins at 9-months of age (52). In addition, animals exhibit stunted growth and a high mortality rate during the first 2 weeks of life caused by the incapacity to feed due to esophagus hyperplasia. This hyperplasia is characterized by an expansion of the keratin 10-positive basal layer of cells and is found in several additional sites, including the skin, palate, forestomach and exocervix (52).

The expression of claudin-1 in the cervix of FvB mice, without E_2 treatment, was higher at the most superficial cell layer facing the lumen, while the presence at the basal cell layers augments, as the age of the mice increases from 2- to 7-months of age, in the present study. This same pattern of expression was found in FvB mice treated with E_2, and in K14E7 mice treated with or without E_2. However, in 2-month-old K14E7 mice treated without E_2 the amount of claudin-1 found in the cervix was higher compared with that in the other experimental groups. On the other hand, the expression of claudin-1 was reduced compared with that in the rest of the cervix in the invasive papillomas that developed in 7-month-old K14E7 mice treated with E_2. These results are consistent with previous research which shows that claudin-1 is markedly expressed in grades I, II and III of human intraepithelial neoplasias, and in situ carcinomas (53-55), but decreases with progression to the invasive phenotype (56).

In addition, the expression of claudin-1 was found to be low in aggressive colorectal carcinomas (57,58) and in gastric cancer (59,60). In the latter (61), as well as in oral squamous cell carcinomas (62) and thyroid cancer (63), the absence of claudin-1 is associated with poorly differentiated tumors. Both papillary urothelial neoplasms of low malignant potential (PUNLMP) and low-grade urothelial cell carcinoma have a decreased expression level of claudin-1 compared with that in inverted urothelial neoplasms, which almost always exhibit a benign behavior (64). The low expression level of claudin-1 was found to be a predictor of recurrence and poor patient survival in colon cancer (65-67), hepatocellular carcinoma (68,69), thyroid (63) and prostate (70) cancer, lung adenocarcinoma (71), non-small cell lung cancer (72) and PUNLMPs (64). With respect to breast cancer, the expression of claudin-1 was initially associated with the basal-like type, which has a very poor prognosis (73,74). However, a previous study has found that a claudin-1 negative phenotype predicts a high risk of recurrence and mortality in triple-negative breast cancers (75). In addition, a reduction or the total loss of the expression levels of expression claudin-1 was also observed in the group of patients with recurrent breast cancer in comparison to the non-recurrent group, as well as in the lymph node metastasis-positive group (76,77). Taken together, the findings from previous research studies are consistent with the results of the present study, that there is a reduced expression level of claudin-1 in the invasive papillomas in 7-month-old K14E7 mice treated with E_2.

Nevertheless, claudin-1 has also been reported to be overexpressed in several cancerous tissues, including high-grade cervical intraepithelial neoplasias (78) and invasive cervical cancer (79), where it has been considered as a biomarker of the disease (80), with a prognosis potential (81). Claudin-1 was also found to be overexpressed in colorectal tumors (82-84), mucoepidermoid carcinomas of the salivary gland (85), thyroid papillary carcinomas, papillary microcarcinomas primary tumors and lymph node metastases (86), and esophageal (87,88), hypopharyngeal (89,90), tongue (91) and oral (92) squamous cell carcinomas, where claudin-1 was found to be associated with cell invasion and disease recurrence (93). Claudin-1 expression in melanoma cells promotes the secretion and activation of metalloproteinase 2, which enhances cell motility (94,95) and mediates tumor necrosis factor α-induced cell migration in gastric cancer cells (96). Claudin-1 was also found to be a prognostic marker and shorter patient survival in kidney clear cell carcinomas (97), intestinal-type gastric cancer (98), lung adenocarcinoma (99) and stage N2 non-small cell lung cancer (100).

The localization of claudin-1 is also altered in cancerous cells. For example, in colorectal cancer, the membrane staining intensity of claudin-1 was reduced compared with that in adjacent non-neoplastic tissue, while a significant increase in claudin-1 cytoplasmic staining was found in colorectal cancer tissue (101). Similarly, in follicular thyroid carcinoma there was negative claudin-1 staining in the membrane and an increase in the nucleus, resulting in increased cell migration and invasion (102). This expression is abnormal as benign thyroid tissue and peritumoral non-malignant thyroid tissue are negative for claudin-1 staining (103,104) and in normal epithelia, in which claudin-1 is expressed [such as the skin (105), kidney (106) and intestine (107,108)], the expression is negative in the nucleus and concentrates at the TJ in the lateral membrane. Thus, evidence is emerging showing that in human cancer, the expression and localization of claudin-1 is altered when compared with that in normal tissue, which was consistent with the results in the murine cervical cancer model in the present study.

It was found in the current study that the expression of claudin-10 in the cervix of FvB mice, without E_2 treatment, was reduced after 2-months of age and was found to be increased in the border of cells in the upper cell layers from the 2-month of age in FvB mice treated with E_2, and in K14E7 mice with and without E_2 treatment. The quantitative analysis of the fluorescence revealed lower values of claudin-10 in

K14E7 mice treated with or without E_2 in the second month of life compared with that in FvB mice treated with E_2; however, this effect was not confirmed using western blot analysis. The reason for this discrepancy remains unknown, although it could be due to the greater statistical variance of the western blots results, which makes them not statistically significant.

Furthermore, in 7-month-old transgenic K14E7 mice treated with E_2, the expression level of claudin-10 in the papillomas, which invades the stroma, was not detectable. This was consistent with previous research which found that the expression of claudin-10 diminishes in breast (109) and biliary tract carcinomas compared with that in normal tissues (110). Moreover, the expression of claudin-10 was associated with the overall survival of patients with lung adenocarcinoma, as it was found to be lower in invasive lepidic adenocarcinoma compared with that in the in situ lung adenocarcinomas (111).

In contrast, the mRNA expression level of claudin-10 was found to be associated with the recurrence of primary hepatocellular carcinoma following curative hepatectomy (112). In addition, type III hepatic tumors with a high malignant potential, display cytoplasmic staining of claudin-10 around the nucleus (113). In the thyroid, claudin-10 was found to be negatively expressed in follicular thyroid carcinomas, and overexpressed in papillary thyroid carcinomas (114), where it serves as a biomarker to distinguish tumors from benign thyroid lesions (115).

With respect to the paracellular permeability of the cervix, treatment of FvB mice with E_2 increased the permeability of TJ to ruthenium red. However, the effect was markedly higher in K14E7 mice treated with or without E_2, which suggest that both E_2 and E7 induce the development of weaker TJs. In this respect, we have previously found that in the skin of ovariectomized FvB mice, E_2 treatment diminishes the expression of TJ proteins occludin and ZO-2 (39). Notably, in mice the blockade of ruthenium red paracellular passage can be established at the most superficial layer of cells in the cervix, while in the human cervix the epithelial junctions that restrict the diffusion of paracellular markers are localized in the cells located three or four layers below the lumen (116).

Following the investigation of the cervix in the transgenic mice, further analysis was performed to determine if the expression of E7 altered the TJs and transformed the characteristics of the normal epithelia, which required transfection of E7 into an epithelial cell line. A non-cancerous cell line of cervix from a mouse or other mammal was not used as to the best of our knowledge these are not currently commercially available. In addition, from the seminal study of TJs in MDCK cells performed by Cereijido *et al* (117) in 1978, the cell line has been widely used to investigate the electrical properties of TJs, the permeability of the paracellular pathway (118-120), the changes in the ultrastructure of TJs visualized in freeze-fracture replicas (38,121), the molecular composition of TJs (46,122-126), as well as the response of TJs to a wide variety of factors, including temperature (127), ions (128-130), signaling cascades (131,132), toxins (133) and growth factors (134,135). Moreover, the role of claudins, in particular claudins -1 (136,137), -2 (46,125,138), -4 (46,125,126) and -10 (33,139) has been extensively studied in MDCK cells. Furthermore, the effect of numerous viruses and viral proteins on TJs has also been investigated in MDCK cells (39-43,140-160). Therefore, the MDCK cell line was selected as it is an ideal *in vitro* model system to investigate factors that regulate or have a harmful effect on TJs.

A stable MDCK cell line was created which expressed E7, and it was found that the monolayers had widened intercellular spaces and had areas in which some cells were growing on top of one another. A similar phenotype was observed in MDCK monolayers where the expression of the TJ protein ZO-2 was knocked down (161,162), which suggests that the E7 oncoprotein exerts a harmful effect on TJs. However, when the development of TER in MDCK-E7 monolayers was analyzed it was found that they achieved a higher peak of TER compared with that in parental cells. This unexpected result led to the investigation into the expression pattern of claudins at the time where TER reaches its highest values. It was found that the protein expression level of claudins -1, -2 and -10 decreased, while that of claudin-4 increased in MDCK-E7 monolayers. The alteration of a single type of claudin can modify, in a significant manner, the permeability and transepithelial electrical resistance of a tissue (163). The increased protein expression level of claudin-4 in MDCK-E7 cells was found to be important, as transfection of this protein can function as a cation barrier in MDCK cells and induce a significant decrease in permeability and an increase in TER (46,48). The decreased expression level of claudin-2 in MDCK-E7 monolayers was expected to have a significant effect on TER, as this claudin, which is highly expressed in leaky epithelia, such as the proximal tubule of the kidney (164) and the intestinal crypts (165), functions as a high conductance cation-permeable pore (44,47). Claudin-1 was found to be ubiquitously expressed claudin and *in vitro* overexpression studies reveal that it acts as a barrier, which increases TER (136,137) therefore, decreased expression would not be expected to contribute to the increased TER observed in MDCK-E7 cells. Claudin-10 has been found to be expressed in numerous tissues, including breast (109), biliary tract (110), lung (111), kidney (33) and liver (113). The function of the two major claudin-10 isoforms revealed that while claudin-10a acts as an anion pore in MDCK II cells (166), claudin-10b has no strong ion selectivity in MDCK II cells which exhibit a high expression of claudin-2 that forms cation pores, but instead claudin-10b acts as a strong cation-permeating pore in high resistance MDCK-C7 cells (33). Claudin-10a expression was found to be restricted to the kidney (33), therefore the remaining tissues, including the cervix and those where the mRNA for claudin-10b has been detected (heart, brain, spleen, lung, liver, skeletal muscle, testis, placenta, eye, lymph node, smooth muscle, prostate, thymus, stomach and uterus) are expected to express claudin-10b. However, as none of the available antibodies, including the one used in the present study, discriminate between claudin-10a and -10b, this was not confirmed in the murine cervix or in MDCK cells.

In MDCK cells it was found that the stable expression of E7 also increases cell migration through a 3D scaffold, stiffens the apical cell membrane, induces the appearance of stress fibers, decreases the expression level of claudins -1, -2 and -10, and augments the expression of claudin-4. All these changes suggest that the cell phenotype was transformed. With respect to increased cell migration and altered claudin expression, previous research has found that migration augments upon

overexpression of claudin-2 in lung cancerous cells (167), claudin-4 in ovarian tumor cells (168), claudin-7 in ovarian cancer (169), claudin-8 in prostate cancer cells (170), claudin-10 in papillary thyroid cancer cells (29) and in hepatocellular carcinomas cells (171), and claudin-17 in hepatic cells (172); or upon silencing of claudin-3 (173) and claudin-4 (173) in ovarian cells OV2008, of claudin-6 in human breast epithelium cell line HBL-100 (174), of claudin-7 in clear cell renal cell carcinoma (175), and of claudin-11 in nasopharyngeal carcinoma (176). In MDCK cells migration augments following claudin-2 silencing (156), and in normal mammary epithelial cells as well as in breast and ovarian tumor cells, blocking the second extracellullar loop in claudin-4, with a peptide, which mimics a conserved sequence in this claudin loop, inhibited cell mobility (167,177,178).

With respect to cell stiffening, tumors have long been characterized for being harder compared with that in normal tissue, and while stiffening of the stroma is a crucial factor that favors tumorigenesis (179,180), changes in the tension of the cell have also been observed during cell transformation (51). MDCK cells also acquire a more rigid apical membrane when the TJ proteins ZO-1 and ZO-2 are both knocked out (181). Moreover, cell stiffening, accompanied by the appearance of stress fibers, has been found to be essential to drive breast tumor growth during premalignant stages (51).

In summary, the results from the present study indicate that the oncogenic protein E7 derived from HPV16 induces epithelial cells changes, including in the expression of claudins -1, -2, -4 and -10 and TJ sealing, which are accompanied by changes in cell stiffness, motility and cytoarchitecture, which could be important in the development of tumorigenesis.

Acknowledgements

This study was part of the doctoral dissertation by Perla Yaceli Uc, a student from the Posgrado en Ciencias Biomédicas, Universidad Nacional Autónoma de México, in which she also received a doctoral fellowship from Consejo Nacional de Ciencia y Tecnología (no. 362696).

Funding

This study was supported by grants from the Miguel Alemán Valdés Foundation 2018, and Secretaría de Educación Pública-Center for Research and Advanced Studies, México (grant no. FIDSC2018/33).

Availability of data and materials

All data generated or analyzed during this study are included in this published article.

Authors' contributions

LGM and PG contributed with the conception and design of the study, and analyzed and interpreted the data. PYU, JM, ARS, LA, BCM, MLR. and GR performed the experiments and analyzed and interpretation the data. ROD maintained and treated the FvB and K14E7 transgenic mice. EMCM obtained cervical samples from the aforementioned mice. LS was involved in the design of the experiment for the development of MDCK-E7 cells. RA designed the procedure for the measurements of the nanomechanical properties of the cells. LGM and PYU wrote the manuscript. PG and ROD revised the manuscript critically. All authors read and revised the manuscript, and approved the final version.

Ethics approval and consent to participate

All animal procedures were performed according to international laws and the Mexican Official Norm (approval no. NOM-062-ZOO-1999) and with the approval of the Center of Research and Advanced Studies Institutional Animal Care and Use Committee (approval no. 0193-16).

Patient consent for publication

Not applicable.

Competing interests

The authors declare that they have no competing interests.

References

1. Bray F, Ferlay J, Soerjomataram I, Siegel RL, Torre LA and Jemal A: Global cancer statistics 2018: GLOBOCAN estimates of incidence and mortality worldwide for 36 cancers in 185 countries. CA Cancer J Clin 68: 394-424, 2018.
2. Siegel RL, Miller KD and Jemal A: Cancer statistics, 2020. CA Cancer J Clin 70: 7-30, 2020.
3. Jemal A, Ward EM, Johnson CJ, Cronin KA, Ma J, Ryerson B, Mariotto A, Lake AJ, Wilson R, Sherman RL, *et al*: Annual Report to the Nation on the Status of Cancer, 1975-2014, Featuring Survival. J Natl Cancer Inst 109: 109, 2017.
4. Paavonen J, Naud P, Salmerón J, Wheeler CM, Chow SN, Apter D, Kitchener H, Castellsague X, Teixeira JC, Skinner SR, *et al*; HPV PATRICIA Study Group: Efficacy of human papillomavirus (HPV)-16/18 AS04-adjuvanted vaccine against cervical infection and precancer caused by oncogenic HPV types (PATRICIA): Final analysis of a double-blind, randomised study in young women. Lancet 374: 301-314, 2009.
5. Muñoz JP, Carrillo-Beltrán D, Aedo-Aguilera V, Calaf GM, León O, Maldonado E, Tapia JC, Boccardo E, Ozbun MA and Aguayo F: Tobacco Exposure Enhances Human Papillomavirus 16 Oncogene Expression via EGFR/PI3K/Akt/c-Jun Signaling Pathway in Cervical Cancer Cells. Front Microbiol 9: 3022, 2018.
6. Muñoz N, Franceschi S, Bosetti C, Moreno V, Herrero R, Smith JS, Shah KV, Meijer CJ and Bosch FX; International Agency for Research on Cancer. Multicentric Cervical Cancer Study Group: Role of parity and human papillomavirus in cervical cancer: The IARC multicentric case-control study. Lancet 359: 1093-1101, 2002.
7. Berraho M, Amarti-Riffi A, El-Mzibri M, Bezad R, Benjaafar N, Benideer A, Matar N, Qmichou Z, Abda N, Attaleb M, *et al*: HPV and cofactors for invasive cervical cancer in Morocco: A multicentre case-control study. BMC Cancer 17: 435, 2017.
8. Chung SH, Franceschi S and Lambert PF: Estrogen and ERalpha: Culprits in cervical cancer? Trends Endocrinol Metab 21: 504-511, 2010.
9. Asthana S, Busa V and Labani S: Oral contraceptives use and risk of cervical cancer-A systematic review & meta-analysis. Eur J Obstet Gynecol Reprod Biol 247: 163-175, 2020.
10. Mapanga W, Singh E, Feresu SA and Girdler-Brown B: Treatment of pre- and confirmed cervical cancer in HIV-seropositive women from developing countries: A systematic review. Syst Rev 9: 79, 2020.
11. Du GH, Wang JK, Richards JR and Wang JJ: Genetic polymorphisms in tumor necrosis factor alpha and interleukin-10 are associated with an increased risk of cervical cancer. Int Immunopharmacol 66: 154-161, 2019.

12. Zhang L, Tian S, Pei M, Zhao M, Wang L, Jiang Y, Yang T, Zhao J, Song L and Yang X: Crosstalk between histone modification and DNA methylation orchestrates the epigenetic regulation of the costimulatory factors, Tim-3 and galectin-9, in cervical cancer. Oncol Rep 42: 2655-2669, 2019.
13. List HJ, Patzel V, Zeidler U, Schopen A, Rühl G, Stollwerk J and Klock G: Methylation sensitivity of the enhancer from the human papillomavirus type 16. J Biol Chem 269: 11902-11911, 1994.
14. Chih HJ, Lee AH, Colville L, Binns CW and Xu D: A review of dietary prevention of human papillomavirus-related infection of the cervix and cervical intraepithelial neoplasia. Nutr Cancer 65: 317-328, 2013.
15. Ghosh C, Baker JA, Moysich KB, Rivera R, Brasure JR and McCann SE: Dietary intakes of selected nutrients and food groups and risk of cervical cancer. Nutr Cancer 60: 331-341, 2008.
16. Song S, Liem A, Miller JA and Lambert PF: Human papillomavirus types 16 E6 and E7 contribute differently to carcinogenesis. Virology 267: 141-150, 2000.
17. Werness BA, Levine AJ and Howley PM: Association of human papillomavirus types 16 and 18 E6 proteins with p53. Science 248: 76-79, 1990.
18. Dyson N, Howley PM, Münger K and Harlow E: The human papilloma virus-16 E7 oncoprotein is able to bind to the retinoblastoma gene product. Science 243: 934-937, 1989.
19. Riley RR, Duensing S, Brake T, Münger K, Lambert PF and Arbeit JM: Dissection of human papillomavirus E6 and E7 function in transgenic mouse models of cervical carcinogenesis. Cancer Res 63: 4862-4871, 2003.
20. Brake T, Connor JP, Petereit DG and Lambert PF: Comparative analysis of cervical cancer in women and in a human papillomavirus-transgenic mouse model: Identification of minichromosome maintenance protein 7 as an informative biomarker for human cervical cancer. Cancer Res 63: 8173-8180, 2003.
21. Arbeit JM, Howley PM and Hanahan D: Chronic estrogen-induced cervical and vaginal squamous carcinogenesis in human papillomavirus type 16 transgenic mice. Proc Natl Acad Sci USA 93: 2930-2935, 1996.
22. Brake T and Lambert PF: Estrogen contributes to the onset, persistence, and malignant progression of cervical cancer in a human papillomavirus-transgenic mouse model. Proc Natl Acad Sci USA 102: 2490-2495, 2005.
23. González-Mariscal L, Díaz-Coránguez M and Quirós M: Regulation of tight junctions for therapeutic advanges. In: Cancer Metastasis-Biology and Treatment. Martin TA and Jiang WG (eds). Springer Dondrecht, pp197-246, 2013.
24. González-Mariscal L, Lechuga S and Garay E: Role of tight junctions in cell proliferation and cancer. Prog Histochem Cytochem 42: 1-57, 2007.
25. Birks DK, Kleinschmidt-DeMasters BK, Donson AM, Barton VN, McNatt SA, Foreman NK and Handler MH: Claudin 6 is a positive marker for atypical teratoid/rhabdoid tumors. Brain Pathol 20: 140-150, 2010.
26. Cortés-Malagón EM, Bonilla-Delgado J, Díaz-Chávez J, Hidalgo-Miranda A, Romero-Cordoba S, Uren A, Celik H, McCormick M, Munguía-Moreno JA, Ibarra-Sierra E, *et al*: Gene expression profile regulated by the HPV16 E7 oncoprotein and estradiol in cervical tissue. Virology 447: 155-165, 2013.
27. Seo HW, Rengaraj D, Choi JW, Ahn SE, Song YS, Song G and Han JY: Claudin 10 is a glandular epithelial marker in the chicken model as human epithelial ovarian cancer. Int J Gynecol Cancer 20: 1465-1473, 2010.
28. Huang GW, Ding X, Chen SL and Zeng L: Expression of claudin 10 protein in hepatocellular carcinoma: Impact on survival. J Cancer Res Clin Oncol 137: 1213-1218, 2011.
29. Zhou Y, Xiang J, Bhandari A, Guan Y, Xia E, Zhou X, Wang Y and Wang O: CLDN10 is Associated with Papillary Thyroid Cancer Progression. J Cancer 9: 4712-4717, 2018.
30. Bulut G, Fallen S, Beauchamp EM, Drebing LE, Sun J, Berry DL, Kallakury B, Crum CP, Toretsky JA, Schlegel R, *et al*: Beta-catenin accelerates human papilloma virus type-16 mediated cervical carcinogenesis in transgenic mice. PLoS One 6: e27243, 2011.
31. González-Mariscal L, Garay E and Quirós M: Identification of claudins by western blot and immunofluorescence in different cell lines and tissues. Methods Mol Biol 762: 213-231, 2011.
32. Lee C and Laimins LA: The differentiation-dependent life cycle of human papillomaviruses in keratinocytes. In: The Papillomaviruses. Garcea RL and DiMaio D (eds). Springer US, Boston, MA, pp45-67, 2007.
33. Günzel D, Stuiver M, Kausalya PJ, Haisch L, Krug SM, Rosenthal R, Meij IC, Hunziker W, Fromm M and Müller D: Claudin-10 exists in six alternatively spliced isoforms that exhibit distinct localization and function. J Cell Sci 122: 1507-1517, 2009.
34. Miranda J, Martín-Tapia D, Valdespino-Vázquez Y, Alarcón L, Espejel-Nuñez A, Guzmán-Huerta M, Muñoz-Medina JE, Shibayama M, Chávez-Munguía B, Estrada-Gutiérrez G, *et al*: Syncytiotrophoblast of Placentae from Women with Zika Virus Infection Has Altered Tight Junction Protein Expression and Increased Paracellular Permeability. Cells 8: 8, 2019.
35. Ortega-Olvera JM, Winkler R, Quintanilla-Vega B, Shibayama M, Chávez-Munguía B, Martín-Tapia D, Alarcón L and González-Mariscal L: The organophosphate pesticide methamidophos opens the blood-testis barrier and covalently binds to ZO-2 in mice. Toxicol Appl Pharmacol 360: 257-272, 2018.
36. Gutiérrez J, García-Villa E, Ocadiz-Delgado R, Cortés-Malagón EM, Vázquez J, Roman-Rosales A, Alvarez-Rios E, Celik H, Romano MC, Üren A, *et al*: Human papillomavirus type 16 E7 oncoprotein upregulates the retinoic acid receptor-beta expression in cervical cancer cell lines and K14E7 transgenic mice. Mol Cell Biochem 408: 261-272, 2015.
37. McFarland DC: Preparation of pure cell cultures by cloning. Methods Cell Sci 22: 63-66, 2000.
38. Gonzalez-Mariscal L, Chávez de Ramírez B and Cereijido M: Tight junction formation in cultured epithelial cells (MDCK). J Membr Biol 86: 113-125, 1985.
39. Hernández-Monge J, Garay E, Raya-Sandino A, Vargas-Sierra O, Díaz-Chávez J, Popoca-Cuaya M, Lambert PF, González-Mariscal L and Gariglio P: Papillomavirus E6 oncoprotein up-regulates occludin and ZO-2 expression in ovariectomized mice epidermis. Exp Cell Res 319: 2588-2603, 2013.
40. Latorre IJ, Roh MH, Frese KK, Weiss RS, Margolis B and Javier RT: Viral oncoprotein-induced mislocalization of select PDZ proteins disrupts tight junctions and causes polarity defects in epithelial cells. J Cell Sci 118: 4283-4293, 2005.
41. Ramirez L, Betanzos A, Raya-Sandino A, González-Mariscal L and Del Angel RM: Dengue virus enters and exits epithelial cells through both apical and basolateral surfaces and perturbs the apical junctional complex. Virus Res 258: 39-49, 2018.
42. Nava P, López S, Arias CF, Islas S and González-Mariscal L: The rotavirus surface protein VP8 modulates the gate and fence function of tight junctions in epithelial cells. J Cell Sci 117: 5509-5519, 2004.
43. Svensson L, Finlay BB, Bass D, von Bonsdorff CH and Greenberg HB: Symmetric infection of rotavirus on polarized human intestinal epithelial (Caco-2) cells. J Virol 65: 4190-4197, 1991.
44. Amasheh S, Meiri N, Gitter AH, Schöneberg T, Mankertz J, Schulzke JD and Fromm M: Claudin-2 expression induces cation-selective channels in tight junctions of epithelial cells. J Cell Sci 115: 4969-4976, 2002.
45. Yu AS, Cheng MH, Angelow S, Günzel D, Kanzawa SA, Schneeberger EE, Fromm M and Coalson RD: Molecular basis for cation selectivity in claudin-2-based paracellular pores: Identification of an electrostatic interaction site. J Gen Physiol 133: 111-127, 2009.
46. Van Itallie CM, Fanning AS and Anderson JM: Reversal of charge selectivity in cation or anion-selective epithelial lines by expression of different claudins. Am J Physiol Renal Physiol 285: F1078-F1084, 2003.
47. Furuse M, Furuse K, Sasaki H and Tsukita S: Conversion of zonulae occludentes from tight to leaky strand type by introducing claudin-2 into Madin-Darby canine kidney I cells. J Cell Biol 153: 263-272, 2001.
48. Van Itallie C, Rahner C and Anderson JM: Regulated expression of claudin-4 decreases paracellular conductance through a selective decrease in sodium permeability. J Clin Invest 107: 1319-1327, 2001.
49. Hou J, Renigunta A, Yang J and Waldegger S: Claudin-4 forms paracellular chloride channel in the kidney and requires claudin-8 for tight junction localization. Proc Natl Acad Sci USA 107: 18010-18015, 2010.
50. Chaicharoenaudomrung N, Kunhorm P and Noisa P: Three-dimensional cell culture systems as an in vitro platform for cancer and stem cell modeling. World J Stem Cells 11: 1065-1083, 2019.
51. Tavares S, Vieira AF, Taubenberger AV, Araújo M, Martins NP, Brás-Pereira C, Polónia A, Herbig M, Barreto C, Otto O, *et al*: Actin stress fiber organization promotes cell stiffening and proliferation of pre-invasive breast cancer cells. Nat Commun 8: 15237, 2017.

52. Herber R, Liem A, Pitot H and Lambert PF: Squamous epithelial hyperplasia and carcinoma in mice transgenic for the human papillomavirus type 16 E7 oncogene. J Virol 70: 1873-1881, 1996.
53. Sobel G, Szabó I, Páska C, Kiss A, Kovalszky I, Kádár A, Paulin F and Schaff Z: Changes of cell adhesion and extracellular matrix (ECM) components in cervical intraepithelial neoplasia. Pathol Oncol Res 11: 26-31, 2005.
54. Chen Y, Miller C, Mosher R, Zhao X, Deeds J, Morrissey M, Bryant B, Yang D, Meyer R, Cronin F, *et al*: Identification of cervical cancer markers by cDNA and tissue microarrays. Cancer Res 63: 1927-1935, 2003.
55. Zinner B, Gyöngyösi B, Babarczi E, Kiss A and Sobel G: Claudin 1 expression characterizes human uterine cervical reserve cells. J Histochem Cytochem 61: 880-888, 2013.
56. Sobel G, Páska C, Szabó I, Kiss A, Kádár A and Schaff Z: Increased expression of claudins in cervical squamous intraepithelial neoplasia and invasive carcinoma. Hum Pathol 36: 162-169, 2005.
57. Ersoz S, Mungan S, Cobanoglu U, Turgutalp H and Ozoran Y: Prognostic importance of Claudin-1 and Claudin-4 expression in colon carcinomas. Pathol Res Pract 207: 285-289, 2011.
58. Süren D, Yıldırım M, Kaya V, Alikanoğlu AS, Bülbüller N, Yıldız M and Sezer C: Loss of tight junction proteins (Claudin 1, 4, and 7) correlates with aggressive behavior in colorectal carcinoma. Med Sci Monit 20: 1255-1262, 2014.
59. Jung H, Jun KH, Jung JH, Chin HM and Park WB: The expression of claudin-1, claudin-2, claudin-3, and claudin-4 in gastric cancer tissue. J Surg Res 167: e185-e191, 2011.
60. Wang H and Yang X: The expression patterns of tight junction protein claudin-1, -3, and -4 in human gastric neoplasms and adjacent non-neoplastic tissues. Int J Clin Exp Pathol 8: 881-887, 2015.
61. Tokuhara Y, Morinishi T, Matsunaga T, Ohsaki H, Kushida Y, Haba R and Hirakawa E: Claudin-1, but not claudin-4, exhibits differential expression patterns between well- to moderately-differentiated and poorly-differentiated gastric adenocarcinoma. Oncol Lett 10: 93-98, 2015.
62. Lourenço SV, Coutinho-Camillo CM, Buim ME, Pereira CM, Carvalho AL, Kowalski LP and Soares FA: Oral squamous cell carcinoma: Status of tight junction claudins in the different histopathological patterns and relationship with clinical parameters. A tissue-microarray-based study of 136 cases. J Clin Pathol 63: 609-614, 2010.
63. Tzelepi VN, Tsamandas AC, Vlotinou HD, Vagianos CE and Scopa CD: Tight junctions in thyroid carcinogenesis: Diverse expression of claudin-1, claudin-4, claudin-7 and occludin in thyroid neoplasms. Mod Pathol 21: 22-30, 2008.
64. Székely E, Törzsök P, Riesz P, Korompay A, Fintha A, Székely T, Lotz G, Nyirády P, Romics I, Tímár J, *et al*: Expression of claudins and their prognostic significance in noninvasive urothelial neoplasms of the human urinary bladder. J Histochem Cytochem 59: 932-941, 2011.
65. Resnick MB, Konkin T, Routhier J, Sabo E and Pricolo VE: Claudin-1 is a strong prognostic indicator in stage II colonic cancer: A tissue microarray study. Mod Pathol 18: 511-518, 2005.
66. Shibutani M, Noda E, Maeda K, Nagahara H, Ohtani H and Hirakawa K: Low expression of claudin-1 and presence of poorly-differentiated tumor clusters correlate with poor prognosis in colorectal cancer. Anticancer Res 33: 3301-3306, 2013.
67. Jiang L, Yang L, Huang H, Liu BY and Zu G: Prognostic and clinical significance of claudin-1 in colorectal cancer: A systemic review and meta-analysis. Int J Surg 39: 214-220, 2017.
68. Higashi Y, Suzuki S, Sakaguchi T, Nakamura T, Baba S, Reinecker HC, Nakamura S and Konno H: Loss of claudin-1 expression correlates with malignancy of hepatocellular carcinoma. J Surg Res 139: 68-76, 2007.
69. Bouchagier KA, Assimakopoulos SF, Karavias DD, Maroulis I, Tzelepi V, Kalofonos H, Karavias DD, Kardamakis D, Scopa CD and Tsamandas AC: Expression of claudins-1, -4, -5, -7 and occludin in hepatocellular carcinoma and their relation with classic clinicopathological features and patients' survival. In Vivo 28: 315-326, 2014.
70. Sheehan GM, Kallakury BV, Sheehan CE, Fisher HA, Kaufman RP Jr and Ross JS: Loss of claudins-1 and -7 and expression of claudins-3 and -4 correlate with prognostic variables in prostatic adenocarcinomas. Hum Pathol 38: 564-569, 2007.
71. Chao YC, Pan SH, Yang SC, Yu SL, Che TF, Lin CW, Tsai MS, Chang GC, Wu CH, Wu YY, *et al*: Claudin-1 is a metastasis suppressor and correlates with clinical outcome in lung adenocarcinoma. Am J Respir Crit Care Med 179: 123-133, 2009.
72. Moldvay J, Fábián K, Jäckel M, Németh Z, Bogos K, Furák J, Tiszlavicz L, Fillinger J, Döme B and Schaff Z: Claudin-1 Protein Expression Is a Good Prognostic Factor in Non-Small Cell Lung Cancer, but only in Squamous Cell Carcinoma Cases. Pathol Oncol Res 23: 151-156, 2017.
73. Blanchard AA, Skliris GP, Watson PH, Murphy LC, Penner C, Tomes L, Young TL, Leygue E and Myal Y: Claudins 1, 3, and 4 protein expression in ER negative breast cancer correlates with markers of the basal phenotype. Virchows Arch 454: 647-656, 2009.
74. Kulka J, Szász AM, Németh Z, Madaras L, Schaff Z, Molnár IA and Tokés AM: Expression of tight junction protein claudin-4 in basal-like breast carcinomas. Pathol Oncol Res 15: 59-64, 2009.
75. Ma F, Ding X, Fan Y, Ying J, Zheng S, Lu N and Xu B: A CLDN1-negative phenotype predicts poor prognosis in triple-negative breast cancer. PLoS One 9: e112765, 2014.
76. Morohashi S, Kusumi T, Sato F, Odagiri H, Chiba H, Yoshihara S, Hakamada K, Sasaki M and Kijima H: Decreased expression of claudin-1 correlates with recurrence status in breast cancer. Int J Mol Med 20: 139-143, 2007.
77. Szasz AM, Tokes AM, Micsinai M, Krenacs T, Jakab C, Lukacs L, Nemeth Z, Baranyai Z, Dede K, Madaras L, *et al*: Prognostic significance of claudin expression changes in breast cancer with regional lymph node metastasis. Clin Exp Metastasis 28: 55-63, 2011.
78. Steinau M, Rajeevan MS, Lee DR, Ruffin MT, Horowitz IR, Flowers LC, Tadros T, Birdsong G, Husain M, Kmak DC, *et al*: Evaluation of RNA markers for early detection of cervical neoplasia in exfoliated cervical cells. Cancer Epidemiol Biomarkers Prev 16: 295-301, 2007.
79. Vázquez-Ortíz G, Ciudad CJ, Piña P, Vazquez K, Hidalgo A, Alatorre B, Garcia JA, Salamanca F, Peralta-Rodriguez R, Rangel A, *et al*: Gene identification by cDNA arrays in HPV-positive cervical cancer. Arch Med Res 36: 448-458, 2005.
80. Benczik M, Galamb Á, Koiss R, Kovács A, Járay B, Székely T, Szekerczés T, Schaff Z, Sobel G and Jeney C: Claudin-1 as a Biomarker of Cervical Cytology and Histology. Pathol Oncol Res 22: 179-188, 2016.
81. Hoellen F, Waldmann A, Banz-Jansen C, Holtrich U, Karn T, Oberländer M, Habermann JK, Hörmann M, Köster F, Ribbat-Idel J, *et al*: Claudin-1 expression in cervical cancer. Mol Clin Oncol 7: 880-884, 2017.
82. Gröne J, Weber B, Staub E, Heinze M, Klaman I, Pilarsky C, Hermann K, Castanos-Velez E, Röpcke S, Mann B, *et al*: Differential expression of genes encoding tight junction proteins in colorectal cancer: Frequent dysregulation of claudin-1, -8 and -12. Int J Colorectal Dis 22: 651-659, 2007.
83. Kinugasa T, Akagi Y, Yoshida T, Ryu Y, Shiratuchi I, Ishibashi N and Shirouzu K: Increased claudin-1 protein expression contributes to tumorigenesis in ulcerative colitis-associated colorectal cancer. Anticancer Res 30: 3181-3186, 2010.
84. Dhawan P, Singh AB, Deane NG, No Y, Shiou SR, Schmidt C, Neff J, Washington MK and Beauchamp RD: Claudin-1 regulates cellular transformation and metastatic behavior in colon cancer. J Clin Invest 115: 1765-1776, 2005.
85. Aro K, Rosa LE, Bello IO, Soini Y, Mäkitie AA, Salo T and Leivo I: Expression pattern of claudins 1 and 3-an auxiliary tool in predicting behavior of mucoepidermoid carcinoma of salivary gland origin. Virchows Arch 458: 341-348, 2011.
86. Németh J, Németh Z, Tátrai P, Péter I, Somorácz A, Szász AM, Kiss A and Schaff Z: High expression of claudin-1 protein in papillary thyroid tumor and its regional lymph node metastasis. Pathol Oncol Res 16: 19-27, 2010.
87. Gyorffy H: Study of claudins and prognostic factors in some gastrointestinal diseases. Magy Onkol 53: 377-383, 2009 (In Hungarian).
88. Montgomery E, Mamelak AJ, Gibson M, Maitra A, Sheikh S, Amr SS, Yang S, Brock M, Forastiere A, Zhang S, *et al*: Overexpression of claudin proteins in esophageal adenocarcinoma and its precursor lesions. Appl Immunohistochem Mol Morphol 14: 24-30, 2006.
89. Li W, Dong Q, Li L, Zhang Z, Cai X and Pan X: Prognostic significance of claudin-1 and cyclin B1 protein expression in patients with hypopharyngeal squamous cell carcinoma. Oncol Lett 11: 2995-3002, 2016.
90. Li WJ, Zhang ZL, Yu XM, Cai XL, Pan XL and Yang XY: Expression of claudin-1 and its relationship with lymphatic microvessel generation in hypopharyngeal squamous cell carcinoma. Genet Mol Res 14: 11814-11826, 2015.

91. Bello IO, Vilen ST, Niinimaa A, Kantola S, Soini Y and Salo T: Expression of claudins 1, 4, 5, and 7 and occludin, and relationship with prognosis in squamous cell carcinoma of the tongue. Hum Pathol 39: 1212-1220, 2008.
92. Babkair H, Yamazaki M, Uddin MS, Maruyama S, Abé T, Essa A, Sumita Y, Ahsan MS, Swelam W, Cheng J, *et al*: Aberrant expression of the tight junction molecules claudin-1 and zonula occludens-1 mediates cell growth and invasion in oral squamous cell carcinoma. Hum Pathol 57: 51-60, 2016.
93. Sappayatosok K and Phattarataratip E: Overexpression of Claudin-1 is Associated with Advanced Clinical Stage and Invasive Pathologic Characteristics of Oral Squamous Cell Carcinoma. Head Neck Pathol 9: 173-180, 2015.
94. Weeraratna AT, Becker D, Carr KM, Duray PH, Rosenblatt KP, Yang S, Chen Y, Bittner M, Strausberg RL, Riggins GJ, *et al*: Generation and analysis of melanoma SAGE libraries: SAGE advice on the melanoma transcriptome. Oncogene 23: 2264-2274, 2004.
95. Leotlela PD, Wade MS, Duray PH, Rhode MJ, Brown HF, Rosenthal DT, Dissanayake SK, Earley R, Indig FE, Nickoloff BJ, *et al*: Claudin-1 overexpression in melanoma is regulated by PKC and contributes to melanoma cell motility. Oncogene 26: 3846-3856, 2007.
96. Shiozaki A, Shimizu H, Ichikawa D, Konishi H, Komatsu S, Kubota T, Fujiwara H, Okamoto K, Iitaka D, Nakashima S, *et al*: Claudin 1 mediates tumor necrosis factor alpha-induced cell migration in human gastric cancer cells. World J Gastroenterol 20: 17863-17876, 2014.
97. Fritzsche FR, Oelrich B, Johannsen M, Kristiansen I, Moch H, Jung K and Kristiansen G: Claudin-1 protein expression is a prognostic marker of patient survival in renal cell carcinomas. Clin Cancer Res 14: 7035-7042, 2008.
98. Huang J, Li J, Qu Y, Zhang J, Zhang L, Chen X, Liu B and Zhu Z: The expression of claudin 1 correlates with β-catenin and is a prognostic factor of poor outcome in gastric cancer. Int J Oncol 44: 1293-1301, 2014.
99. Sun BS, Yao YQ, Pei BX, Zhang ZF and Wang CL: Claudin-1 correlates with poor prognosis in lung adenocarcinoma. Thorac Cancer 7: 556-563, 2016.
100. Zhang ZF, Pei BX, Wang AL, Zhang LM, Sun BS, Jiang RC and Wang CL: Expressions of CLDN1 and insulin-like growth factor 2 are associated with poor prognosis in stage N2 non-small cell lung cancer. Chin Med J (Engl) 126: 3668-3674, 2013.
101. Hahn-Strömberg V, Askari S, Ahmad A, Befekadu R and Nilsson TK: Expression of claudin 1, claudin 4, and claudin 7 in colorectal cancer and its relation with CLDN DNA methylation patterns. Tumour Biol 39: 1010428317697569, 2017.
102. Zwanziger D, Badziong J, Ting S, Moeller LC, Schmid KW, Siebolts U, Wickenhauser C, Dralle H and Fuehrer D: The impact of CLAUDIN-1 on follicular thyroid carcinoma aggressiveness. Endocr Relat Cancer 22: 819-830, 2015.
103. Ma H, Yan J, Zhang C, Qin S, Qin L, Liu L, Wang X and Li N: Expression of papillary thyroid carcinoma-associated molecular markers and their significance in follicular epithelial dysplasia with papillary thyroid carcinoma-like nuclear alterations in Hashimoto's thyroiditis. Int J Clin Exp Pathol 7: 7999-8007, 2014.
104. Abd El Atti RM and Shash LS: Potential diagnostic utility of CD56 and claudin-1 in papillary thyroid carcinoma and solitary follicular thyroid nodules. J Egypt Natl Canc Inst 24: 175-184, 2012.
105. Furuse M, Hata M, Furuse K, Yoshida Y, Haratake A, Sugitani Y, Noda T, Kubo A and Tsukita S: Claudin-based tight junctions are crucial for the mammalian epidermal barrier: A lesson from claudin-1-deficient mice. J Cell Biol 156: 1099-1111, 2002.
106. Reyes JL, Lamas M, Martin D, del Carmen Namorado M, Islas S, Luna J, Tauc M and González-Mariscal L: The renal segmental distribution of claudins changes with development. Kidney Int 62: 476-487, 2002.
107. Lu Z, Ding L, Lu Q and Chen YH: Claudins in intestines: Distribution and functional significance in health and diseases. Tissue Barriers 1: e24978, 2013.
108. Garcia-Hernandez V, Quiros M and Nusrat A: Intestinal epithelial claudins: Expression and regulation in homeostasis and inflammation. Ann N Y Acad Sci 1397: 66-79, 2017.
109. Tőkés AM, Szász AM, Juhász E, Schaff Z, Harsányi L, Molnár IA, Baranyai Z, Besznyák I Jr, Zaránd A, Salamon F, *et al*: Expression of tight junction molecules in breast carcinomas analysed by array PCR and immunohistochemistry. Pathol Oncol Res 18: 593-606, 2012.
110. Németh Z, Szász AM, Tátrai P, Németh J, Gyorffy H, Somorácz A, Szíjártó A, Kupcsulik P, Kiss A and Schaff Z: Claudin-1, -2, -3, -4, -7, -8, and -10 protein expression in biliary tract cancers. J Histochem Cytochem 57: 113-121, 2009.
111. Zhang Z, Wang A, Sun B, Zhan Z, Chen K and Wang C: Expression of CLDN1 and CLDN10 in lung adenocarcinoma in situ and invasive lepidic predominant adenocarcinoma. J Cardiothorac Surg 8: 95, 2013.
112. Cheung ST, Leung KL, Ip YC, Chen X, Fong DY, Ng IO, Fan ST and So S: Claudin-10 expression level is associated with recurrence of primary hepatocellular carcinoma. Clin Cancer Res 11: 551-556, 2005.
113. Sanada Y, Yoshida K and Itoh H: Comparison of CT enhancement patterns and histologic features in hepatocellular carcinoma up to 2 cm: Assessment of malignant potential with claudin-10 immunohistochemistry. Oncol Rep 17: 1177-1182, 2007.
114. Aldred MA, Huang Y, Liyanarachchi S, Pellegata NS, Gimm O, Jhiang S, Davuluri RV, de la Chapelle A and Eng C: Papillary and follicular thyroid carcinomas show distinctly different microarray expression profiles and can be distinguished by a minimum of five genes. J Clin Oncol 22: 3531-3539, 2004.
115. Barros-Filho MC, Marchi FA, Pinto CA, Rogatto SR and Kowalski LP: High Diagnostic Accuracy Based on CLDN10, HMGA2, and LAMB3 Transcripts in Papillary Thyroid Carcinoma. J Clin Endocrinol Metab 100: E890-E899, 2015.
116. Blaskewicz CD, Pudney J and Anderson DJ: Structure and function of intercellular junctions in human cervical and vaginal mucosal epithelia. Biol Reprod 85: 97-104, 2011.
117. Cereijido M, Robbins ES, Dolan WJ, Rotunno CA and Sabatini DD: Polarized monolayers formed by epithelial cells on a permeable and translucent support. J Cell Biol 77: 853-880, 1978.
118. Martinez-Palomo A, Meza I, Beaty G and Cereijido M: Experimental modulation of occluding junctions in a cultured transporting epithelium. J Cell Biol 87: 736-745, 1980.
119. Meza I, Ibarra G, Sabanero M, Martínez-Palomo A and Cereijido M: Occluding junctions and cytoskeletal components in a cultured transporting epithelium. J Cell Biol 87: 746-754, 1980.
120. Meza I, Sabanero M, Stefani E and Cereijido M: Occluding junctions in MDCK cells: Modulation of transepithelial permeability by the cytoskeleton. J Cell Biochem 18: 407-421, 1982.
121. Cereijido M, Stefani E and Palomo AM: Occluding junctions in a cultured transporting epithelium: Structural and functional heterogeneity. J Membr Biol 53: 19-32, 1980.
122. Balda MS, Whitney JA, Flores C, González S, Cereijido M and Matter K: Functional dissociation of paracellular permeability and transepithelial electrical resistance and disruption of the apical-basolateral intramembrane diffusion barrier by expression of a mutant tight junction membrane protein. J Cell Biol 134: 1031-1049, 1996.
123. Fanning AS, Little BP, Rahner C, Utepbergenov D, Walther Z and Anderson JM: The unique-5 and -6 motifs of ZO-1 regulate tight junction strand localization and scaffolding properties. Mol Biol Cell 18: 721-731, 2007.
124. Van Itallie CM, Gambling TM, Carson JL and Anderson JM: Palmitoylation of claudins is required for efficient tight-junction localization. J Cell Sci 118: 1427-1436, 2005.
125. Colegio OR, Van Itallie C, Rahner C and Anderson JM: Claudin extracellular domains determine paracellular charge selectivity and resistance but not tight junction fibril architecture. Am J Physiol Cell Physiol 284: C1346-C1354, 2003.
126. Colegio OR, Van Itallie CM, McCrea HJ, Rahner C and Anderson JM: Claudins create charge-selective channels in the paracellular pathway between epithelial cells. Am J Physiol Cell Physiol 283: C142-C147, 2002.
127. González-Mariscal L, Chávez de Ramírez B and Cereijido M: Effect of temperature on the occluding junctions of monolayers of epithelioid cells (MDCK). J Membr Biol 79: 175-184, 1984.
128. Gonzalez-Mariscal L, Contreras RG, Bolívar JJ, Ponce A, Chávez De Ramirez B and Cereijido M: Role of calcium in tight junction formation between epithelial cells. Am J Physiol 259: C978-C986, 1990.
129. Contreras RG, Miller JH, Zamora M, González-Mariscal L and Cereijido M: Interaction of calcium with plasma membrane of epithelial (MDCK) cells during junction formation. Am J Physiol 263: C313-C318, 1992.

130. Amaya E, Alarcón L, Martín-Tapia D, Cuellar-Pérez F, Cano-Cortina M, Ortega-Olvera JM, Cisneros B, Rodriguez AJ, Gamba G and González-Mariscal L: Activation of the Ca^{2+} sensing receptor and the PKC/WNK4 downstream signaling cascade induces incorporation of ZO-2 to tight junctions and its separation from 14-3-3. Mol Biol Cell 30: 2377-2398, 2019.
131. Balda MS, Gonzalez-Mariscal L, Matter K, Cereijido M and Anderson JM: Assembly of the tight junction: The role of diacylglycerol. J Cell Biol 123: 293-302, 1993.
132. Balda MS, González-Mariscal L, Contreras RG, Macias-Silva M, Torres-Marquez ME, García-Sáinz JA and Cereijido M: Assembly and sealing of tight junctions: Possible participation of G-proteins, phospholipase C, protein kinase C and calmodulin. J Membr Biol 122: 193-202, 1991.
133. Sonoda N, Furuse M, Sasaki H, Yonemura S, Katahira J, Horiguchi Y and Tsukita S: Clostridium perfringens enterotoxin fragment removes specific claudins from tight junction strands: Evidence for direct involvement of claudins in tight junction barrier. J Cell Biol 147: 195-204, 1999.
134. Feldman G, Kiely B, Martin N, Ryan G, McMorrow T and Ryan MP: Role for TGF-beta in cyclosporine-induced modulation of renal epithelial barrier function. J Am Soc Nephrol 18: 1662-1671, 2007.
135. García-Hernández V, Flores-Maldonado C, Rincon-Heredia R, Verdejo-Torres O, Bonilla-Delgado J, Meneses-Morales I, Gariglio P and Contreras RG: EGF regulates claudin-2 and -4 expression through Src and STAT3 in MDCK cells. J Cell Physiol 230: 105-115, 2015.
136. Inai T, Kobayashi J and Shibata Y: Claudin-1 contributes to the epithelial barrier function in MDCK cells. Eur J Cell Biol 78: 849-855, 1999.
137. McCarthy KM, Francis SA, McCormack JM, Lai J, Rogers RA, Skare IB, Lynch RD and Schneeberger EE: Inducible expression of claudin-1-myc but not occludin-VSV-G results in aberrant tight junction strand formation in MDCK cells. J Cell Sci 113: 3387-3398, 2000.
138. Van Itallie CM, Mitic LL and Anderson JM: Claudin-2 forms homodimers and is a component of a high molecular weight protein complex. J Biol Chem 286: 3442-3450, 2011.
139. Milatz S, Piontek J, Hempel C, Meoli L, Grohe C, Fromm A, Lee IM, El-Athman R and Günzel D: Tight junction strand formation by claudin-10 isoforms and claudin-10a/-10b chimeras. Ann N Y Acad Sci 1405: 102-115, 2017.
140. Nakagawa S and Huibregtse JM: Human scribble (Vartul) is targeted for ubiquitin-mediated degradation by the high-risk papillomavirus E6 proteins and the E6AP ubiquitin-protein ligase. Mol Cell Biol 20: 8244-8253, 2000.
141. Golebiewski L, Liu H, Javier RT and Rice AP: The avian influenza virus NS1 ESEV PDZ binding motif associates with Dlg1 and Scribble to disrupt cellular tight junctions. J Virol 85: 10639-10648, 2011.
142. Johnson C, Sanders K and Fan H: Jaagsiekte sheep retrovirus transformation in Madin-Darby canine kidney epithelial cell three-dimensional culture. J Virol 84: 5379-5390, 2010.
143. Töyli M, Rosberg-Kulha L, Capra J, Vuoristo J and Eskelinen S: Different responses in transformation of MDCK cells in 2D and 3D culture by v-Src as revealed by microarray techniques, RT-PCR and functional assays. Lab Invest 90: 915-928, 2010.
144. Mettlen M, Platek A, Van Der Smissen P, Carpentier S, Amyere M, Lanzetti L, de Diesbach P, Tyteca D and Courtoy PJ: Src triggers circular ruffling and macropinocytosis at the apical surface of polarized MDCK cells. Traffic 7: 589-603, 2006.
145. Rahikkala M, Sormunen R and Eskelinen S: Effects of src kinase and TGFbeta1 on the differentiation and morphogenesis of MDCK cells grown in three-dimensional collagen and Matrigel environments. J Pathol 195: 391-400, 2001.
146. Tsukamoto T and Nigam SK: Cell-cell dissociation upon epithelial cell scattering requires a step mediated by the proteasome. J Biol Chem 274: 24579-24584, 1999.
147. Takeda H and Tsukita S: Effects of tyrosine phosphorylation on tight junctions in temperature-sensitive v-src-transfected MDCK cells. Cell Struct Funct 20: 387-393, 1995.
148. Connolly-Andersen AM, Magnusson KE and Mirazimi A: Basolateral entry and release of Crimean-Congo hemorrhagic fever virus in polarized MDCK-1 cells. J Virol 81: 2158-2164, 2007.
149. Nunbhakdi-Craig V, Craig L, Machleidt T and Sontag E: Simian virus 40 small tumor antigen induces deregulation of the actin cytoskeleton and tight junctions in kidney epithelial cells. J Virol 77: 2807-2818, 2003.
150. Tafazoli F, Zeng CQ, Estes MK, Magnusson KE and Svensson L: NSP4 enterotoxin of rotavirus induces paracellular leakage in polarized epithelial cells. J Virol 75: 1540-1546, 2001.
151. Mo C, Schneeberger EE and Arvin AM: Glycoprotein E of varicella-zoster virus enhances cell-cell contact in polarized epithelial cells. J Virol 74: 11377-11387, 2000.
152. Rajasekaran AK, Hojo M, Huima T and Rodriguez-Boulan E: Catenins and zonula occludens-1 form a complex during early stages in the assembly of tight junctions. J Cell Biol 132: 451-463, 1996.
153. Gottlieb TA, Ivanov IE, Adesnik M and Sabatini DD: Actin microfilaments play a critical role in endocytosis at the apical but not the basolateral surface of polarized epithelial cells. J Cell Biol 120: 695-710, 1993.
154. Stephens EB, Compans RW, Earl P and Moss B: Surface expression of viral glycoproteins is polarized in epithelial cells infected with recombinant vaccinia viral vectors. EMBO J 5: 237-245, 1986.
155. Schoenenberger CA, Zuk A, Kendall D and Matlin KS: Multilayering and loss of apical polarity in MDCK cells transformed with viral K-ras. J Cell Biol 112: 873-889, 1991.
156. Gravotta D, Adesnik M and Sabatini DD: Transport of influenza HA from the trans-Golgi network to the apical surface of MDCK cells permeabilized in their basolateral plasma membranes: Energy dependence and involvement of GTP-binding proteins. J Cell Biol 111: 2893-2908, 1990.
157. van Meer G and Simons K: The function of tight junctions in maintaining differences in lipid composition between the apical and the basolateral cell surface domains of MDCK cells. EMBO J 5: 1455-1464, 1986.
158. Rindler MJ, Ivanov IE, Plesken H, Rodriguez-Boulan E and Sabatini DD: Viral glycoproteins destined for apical or basolateral plasma membrane domains traverse the same Golgi apparatus during their intracellular transport in doubly infected Madin-Darby canine kidney cells. J Cell Biol 98: 1304-1319, 1984.
159. Roth MG and Compans RW: Delayed appearance of pseudotypes between vesicular stomatitis virus influenza virus during mixed infection of MDCK cells. J Virol 40: 848-860, 1981.
160. Noyce RS, Delpeut S and Richardson CD: Dog nectin-4 is an epithelial cell receptor for canine distemper virus that facilitates virus entry and syncytia formation. Virology 436: 210-220, 2013.
161. Hernandez S, Chavez Munguia B and Gonzalez-Mariscal L: ZO-2 silencing in epithelial cells perturbs the gate and fence function of tight junctions and leads to an atypical monolayer architecture. Exp Cell Res 313: 1533-1547, 2007.
162. Raya-Sandino A, Castillo-Kauil A, Domínguez-Calderón A, Alarcón L, Flores-Benitez D, Cuellar-Perez F, López-Bayghen B, Chávez-Munguía B, Vázquez-Prado J and González-Mariscal L: Zonula occludens-2 regulates Rho proteins activity and the development of epithelial cytoarchitecture and barrier function. Biochim Biophys Acta Mol Cell Res 1864: 1714-1733, 2017.
163. Günzel D and Yu AS: Claudins and the modulation of tight junction permeability. Physiol Rev 93: 525-569, 2013.
164. Enck AH, Berger UV and Yu AS: Claudin-2 is selectively expressed in proximal nephron in mouse kidney. Am J Physiol Renal Physiol 281: F966-F974, 2001.
165. Rahner C, Mitic LL and Anderson JM: Heterogeneity in expression and subcellular localization of claudins 2, 3, 4, and 5 in the rat liver, pancreas, and gut. Gastroenterology 120: 411-422, 2001.
166. Van Itallie CM, Rogan S, Yu A, Vidal LS, Holmes J and Anderson JM: Two splice variants of claudin-10 in the kidney create paracellular pores with different ion selectivities. Am J Physiol Renal Physiol 291: F1288-F1299, 2006.
167. Ikari A, Sato T, Takiguchi A, Atomi K, Yamazaki Y and Sugatani J: Claudin-2 knockdown decreases matrix metalloproteinase-9 activity and cell migration via suppression of nuclear Sp1 in A549 cells. Life Sci 88: 628-633, 2011.
168. Hicks DA, Galimanis CE, Webb PG, Spillman MA, Behbakht K, Neville MC and Baumgartner HK: Claudin-4 activity in ovarian tumor cell apoptosis resistance and migration. BMC Cancer 16: 788, 2016.
169. Dahiya N, Becker KG, Wood WH III, Zhang Y and Morin PJ: Claudin-7 is frequently overexpressed in ovarian cancer and promotes invasion. PLoS One 6: e22119, 2011.
170. Ashikari D, Takayama KI, Obinata D, Takahashi S and Inoue S: CLDN8, an androgen-regulated gene, promotes prostate cancer cell proliferation and migration. Cancer Sci 108: 1386-1393, 2017.

171. Ip YC, Cheung ST, Lee YT, Ho JC and Fan ST: Inhibition of hepatocellular carcinoma invasion by suppression of claudin-10 in HLE cells. Mol Cancer Ther 6: 2858-2867, 2007.
172. Sun L, Feng L and Cui J: Increased expression of claudin-17 promotes a malignant phenotype in hepatocyte via Tyk2/Stat3 signaling and is associated with poor prognosis in patients with hepatocellular carcinoma. Diagn Pathol 13: 72, 2018.
173. Shang X, Lin X, Alvarez E, Manorek G and Howell SB: Tight junction proteins claudin-3 and claudin-4 control tumor growth and metastases. Neoplasia 14: 974-985, 2012.
174. Ren Y, Wu Q, Liu Y, Xu X and Quan C: Gene silencing of claudin-6 enhances cell proliferation and migration accompanied with increased MMP-2 activity via p38 MAPK signaling pathway in human breast epithelium cell line HBL-100. Mol Med Rep 8: 1505-1510, 2013.
175. Li Y, Gong Y, Ning X, Peng D, Liu L, He S, Gong K, Zhang C, Li X and Zhou L: Downregulation of CLDN7 due to promoter hypermethylation is associated with human clear cell renal cell carcinoma progression and poor prognosis. J Exp Clin Cancer Res 37: 276, 2018.
176. Li HP, Peng CC, Wu CC, Chen CH, Shih MJ, Huang MY, Lai YR, Chen YL, Chen TW, Tang P, *et al*: Inactivation of the tight junction gene CLDN11 by aberrant hypermethylation modulates tubulins polymerization and promotes cell migration in nasopharyngeal carcinoma. J Exp Clin Cancer Res 37: 102, 2018.
177. Webb PG, Spillman MA and Baumgartner HK: Claudins play a role in normal and tumor cell motility. BMC Cell Biol 14: 19, 2013.
178. Ikari A, Takiguchi A, Atomi K, Sato T and Sugatani J: Decrease in claudin-2 expression enhances cell migration in renal epithelial Madin-Darby canine kidney cells. J Cell Physiol 226: 1471-1478, 2011.
179. Handorf AM, Zhou Y, Halanski MA and Li WJ: Tissue stiffness dictates development, homeostasis, and disease progression. Organogenesis 11: 1-15, 2015.
180. Indra I and Beningo KA: An in vitro correlation of metastatic capacity, substrate rigidity, and ECM composition. J Cell Biochem 112: 3151-3158, 2011.
181. Cartagena-Rivera AX, Van Itallie CM, Anderson JM and Chadwick RS: Apical surface supracellular mechanical properties in polarized epithelium using noninvasive acoustic force spectroscopy. Nat Commun 8: 1030, 2017.